# Qeios

Research Article

# A Contextual Fear Conditioning Paradigm in Head-Fixed Mice Exploring Virtual Reality

Seetha Krishnan[1], Can Dong[1], Heather Ratigan[1], Denisse Morales-Rodriguez[1], Chery Cherian[1], Mark Sheffield[1]

1. Department of Neurobiology and Institute for Neuroscience, University of Chicago, United States

Contextual fear conditioning is a classical laboratory task that tests associative memory formation and recall. Techniques such as multi-photon microscopy and holographic stimulation offer tremendous opportunities to understand the neural underpinnings of these memories. However, these techniques generally require animals to be head-fixed. There are few paradigms that test contextual fear conditioning in head-fixed mice, and none where the behavioral outcome following fear conditioning is freezing, the most common measure of fear in freely moving animals. To address this gap, we developed a contextual fear conditioning paradigm in head-fixed mice using virtual reality (VR) environments. We designed an apparatus to deliver tail shocks (unconditioned stimulus, US) while mice navigated a VR environment (conditioned stimulus, CS). The acquisition of contextual fear was tested when the mice were reintroduced to the shock-paired VR environment the following day. We tested three different variations of this paradigm and, in all of them, observed an increased conditioned fear response characterized by increased freezing behavior. This was especially prominent during the first trial in the shock-paired VR environment, compared to a neutral environment where the mice received no shocks. Our results demonstrate that head-fixed mice can be fear conditioned in VR, discriminate between a feared and neutral VR context, and display freezing as a conditioned response, similar to freely behaving animals. Furthermore, using a two-photon microscope, we imaged from large populations of hippocampal CA1 neurons before, during, and following contextual fear conditioning. Our findings reconfirmed those from the literature on freely moving animals, showing that CA1 place cells undergo remapping and show narrower place fields following fear conditioning. Our approach offers new opportunities to study the neural mechanisms underlying the formation, recall, and extinction of contextual fear memories. As the head-fixed

preparation is compatible with multi-photon microscopy and holographic stimulation, it enables long-term tracking and manipulation of cells throughout distinct memory stages and provides subcellular resolution for investigating axonal, dendritic, and synaptic dynamics in real-time.

Seetha Krishnan and Can Dong equally contributed to this work.

**Corresponding authors:** Seetha Krishnan, seethakrishnan@uchicago.edu; Mark Sheffield, sheffield@uchicago.edu

# Introduction

Large-scale multi-photon imaging and holographic stimulation offers the ability to accurately track and record from the same neuronal populations over extended periods at high spatiotemporal resolution, record from axons, dendrites, and dendritic spines, and stimulate neurons with single-cell precision[1][2][3][4][5][6][7][8][9][10][11][12]. These techniques facilitate the study of neural circuit dynamics, synaptic and plasticity mechanisms and enable the real-time manipulation of neural activity, all of which are crucial for understanding the mechanisms underlying memory formation and recall in the brain. However, head-fixation of animals, which is generally required to utilize these techniques, imposes constraints on the range of testable behaviors compared to freely moving conditions[13][14]. This limitation is particularly evident in the Pavlovian contextual fear conditioning (CFC) task, a laboratory method for testing associative learning, fear memory formation, and recall[15][16][17][18][19][20][21].

In the traditional CFC paradigm for freely moving animals, an animal is placed in an environment (conditioned stimulus, CS) that is paired with an aversive stimulus, such as a mild foot shock (unconditioned stimulus, US). Animals are then removed from the environment. When reintroduced to the environment, animals exhibit a species-specific conditioned response, such as fearful freezing behavior in rodents, if they successfully associate the shock-paired environment with the aversive stimulus. The CFC paradigm is one of the most basic conditioning procedures for freely moving animals — it's simple and robust[16][17]. Despite its longstanding use in studies involving freely behaving animals to explore questions on learning and memory[22][15][23][24][25][26][27][28][29][30][21][31][32], it has been noticeably absent in studies involving head-fixed animals, with some exceptions.

Two prior studies[33][34] reported a version of CFC in head-fixed mice with aversive air puffs as the US. These studies reported the conditioned response animals displayed as lick suppression, not freezing.

Although lick suppression after fear conditioning has also been observed in freely moving animals[35][36], it has been shown to result from increased freezing[24]. Therefore, relying solely on lick suppression in the head-fixed preparation makes it more challenging to compare with the extensive previous work in freely moving animals, where freezing is measured as the predominant conditioned fear response. Furthermore, the aforementioned head-fixed CFC studies also had the limitation of simultaneously having both a water reward and an aversive stimulus within the context, potentially confounding the results and complicating the interpretation. Hence, we aimed to develop a paradigm where freezing is the conditioned response and without the presence of a reward within the conditioned context, making it directly comparable to freely moving animals.
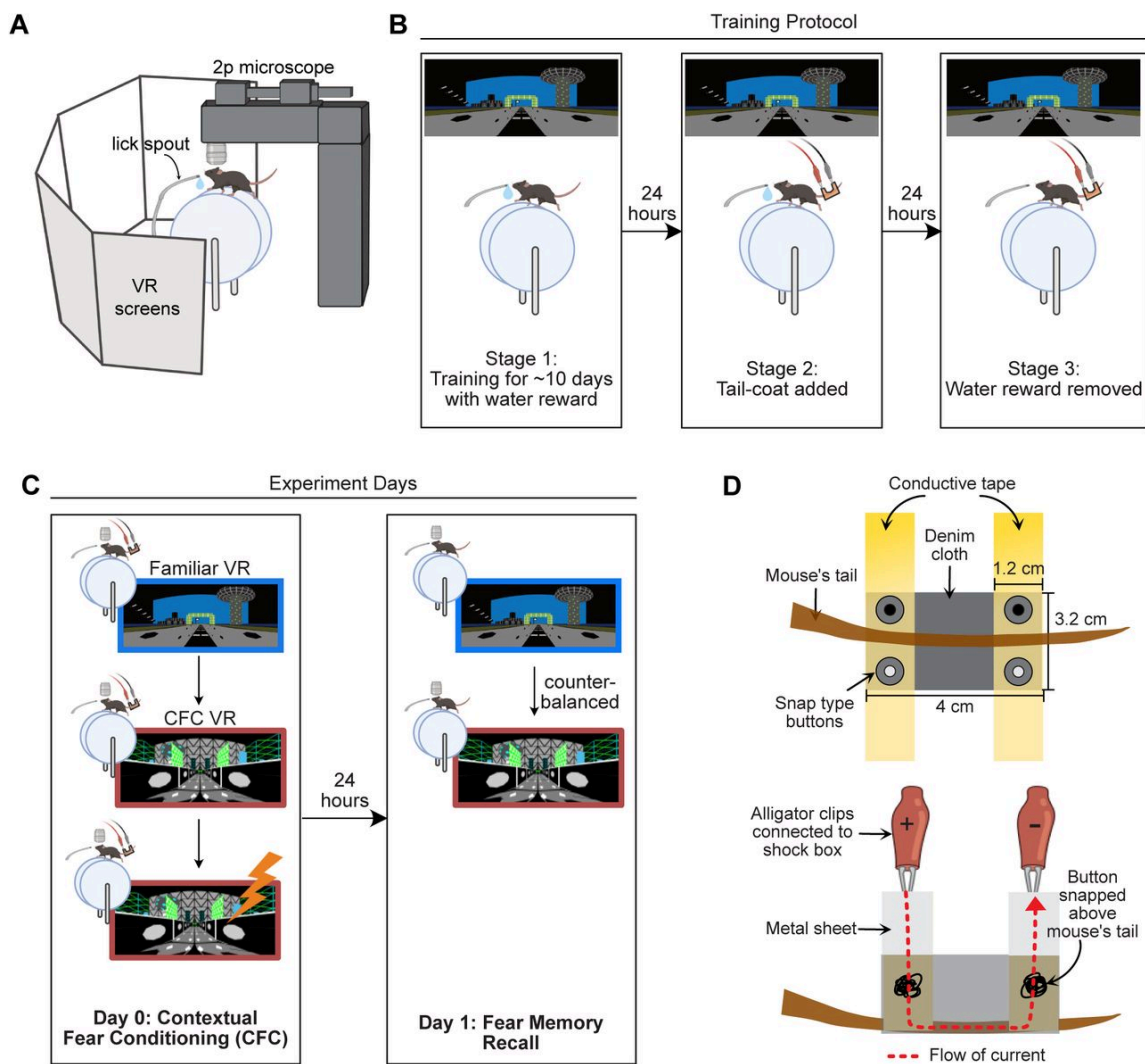
Here, we describe a contextual fear-conditioning paradigm for head-fixed mice that resulted in freezing as the conditioned response. The context or CS was a virtual reality (VR)-based environment, which head-fixed mice explored by running on a spherical treadmill. We previously demonstrated the feasibility of this approach[37] and now provide a detailed overview and in-depth analysis of the behavior. Our main aim is to show that VR-based CFC can elicit freezing responses similar to those seen in freely moving animals, while also examining how key parameters affect this response. Though we explored some important variables, this paper does not attempt to comprehensively investigate all parameters necessary for successful VR-based CFC. Additionally, we performed two-photon imaging of a large population of hippocampal CA1 cells during fear conditioning and tracked the same cells during memory recall across days. We analyzed the impact of our paradigm on place cells in the hippocampus and compared these findings to results from CFC in freely moving animals.

# Results

## *A paradigm for contextual fear conditioning in head-fixed mice exploring virtual reality environments*

To establish the contextual fear conditioning protocol (**Figure 1A–C**), head-fixed mice were water-restricted and trained to run on a treadmill and navigate VR environments for water rewards, as we have demonstrated previously[4][10][38][37]. Forward movement on the treadmill translates to forward movement in VR, allowing mice to navigate the VR environment. The environments used were 2m-long linear tracks rich in visual cues (**Figure 1**). Reaching the track's end triggered a water reward and defined a completed trial/lap. Mice were then virtually teleported back to the track's start for the next lap. Unlike

freely moving mice that tend to explore new environments, head-fixed mice placed on a treadmill do not automatically start exploring VR environments. However, they can be trained through reinforcement learning using water restriction and water rewards[3][4][10][37][12].

**Figure 1. A contextual fear conditioning paradigm for head-fixed mice navigating virtual reality environments.**

**(A)** Experimental setup created with BioRender.com. Mice were head-restrained with their feet resting on a spherical treadmill. Five large monitors surrounded the mice that displayed virtual reality (VR) environments. Movement on the treadmill advanced the VR display, allowing for context exploration.

**(B)** Mice were water-restricted and trained to run laps in the VR for water rewards. VR environments were 2m-long linear tracks. Mice were trained to achieve >3 laps per minute, which took ~10 to 14 days (Stage 1). Once well-trained, a "tail-coat" was added to their tails (Stage 2), followed by the removal of the water reward the next day (Stage 3).

**(C)** Once the water reward was removed, mice underwent the fear conditioning protocol the following day. On the first experiment day (Day 0), mice spent 10 minutes in the training VR (Familiar VR) and then another 10 minutes in a new VR (CFC VR). After the initial exploration, mice received mild electric shocks on the tail (4-12 shocks, 0.5-1.2mA in amplitude, 1s long). The next day (Day 1), mice were tested for memory recall by placing

them in the Familiar VR and the CFC VR for 5 minutes each in a counterbalanced manner.

**(D)** Schematic of the tail-coat used for delivering mild electric shocks to the mouse's tail. (Top) View from the top (Bottom) side view. Dimensions are provided for a typical 12-week-old male mouse weighing ~30g before water restriction (see Methods for more details).

Training to navigate VR environments on a treadmill (Stage 1), using water rewards, was achieved in approximately 10-14 days, after which well-trained mice could run several laps per minute. We set a criterion of >3 laps per minute (i.e., a lap velocity of 0.1 - 0.2 m/s) for mice to move on to the next stage (Stage 2). Once the mice reached this stage (Stage 2), the following day, we added a coat to their tails (**Figure 1B**). We developed a lightweight, wearable conductive apparatus for the mouse's tail to ensure minimal discomfort for the mouse. We named this apparatus the "tail-coat" (**Figure 1D**). This tail- coat enabled us to administer mild electric shocks to the mouse's tail (see Methods).

When the tail-coat was added, some mice reduced their running speed or refused to move. Some recovered the next day, but if their running speed did not reach at least three laps per minute (~20% of mice failed to meet this criterion), they were not advanced to the next stage. Mice that maintained this running speed advanced to Stage 3. Data from mice that advanced with minimal changes to their lap running behavior after adding the tail-coat are shown in **Supplementary Figure 1A**.
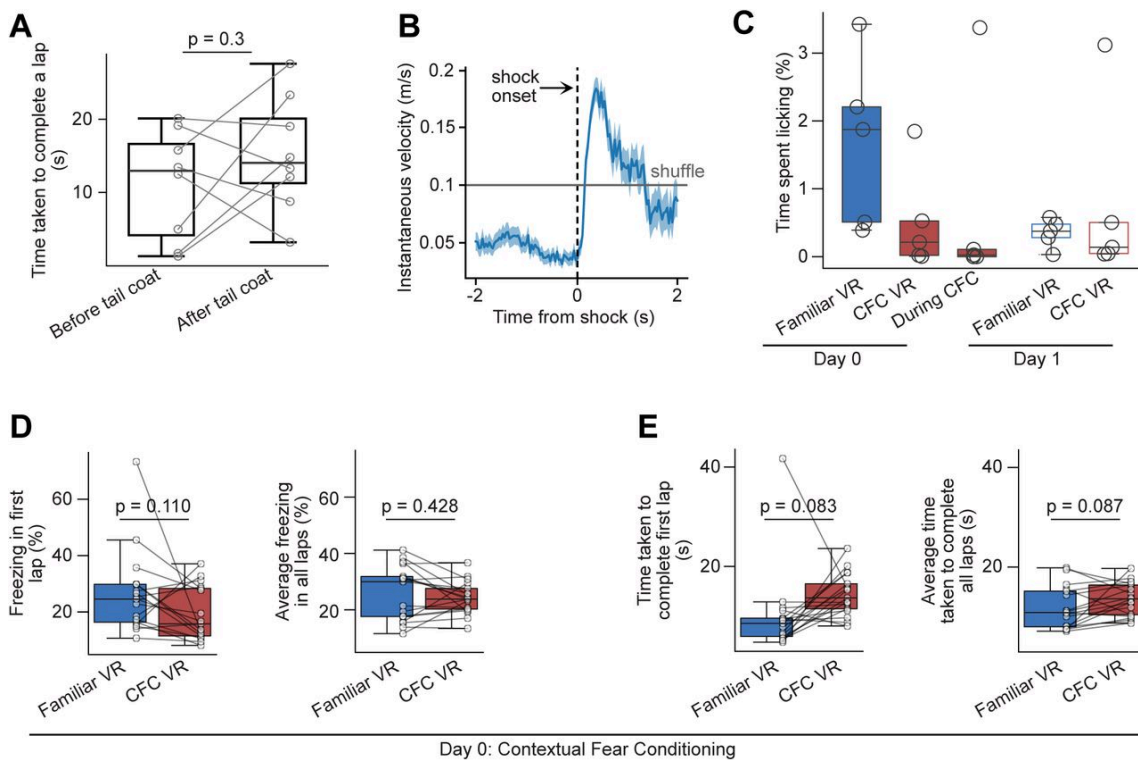
**Supplementary Figure 1. Running and licking behaviors in Paradigm 1.**

**(A)** Box plot of average time taken to complete a lap before and after the addition of a tail-coat recorded in a randomly chosen subset of mice (circles, n=8).

**(B)** Instantaneous velocity increased immediately after shock onset. This increased running speed also served as a reliable measure to confirm that mice received the tail shock. The grey line indicates the average velocity calculated by shuffling the instantaneous velocity 100 times.

**(C)** Licking behavior doesn't stop immediately in the familiar VR without water, as mice previously received water rewards in the familiar VR. However, it was low in the other sessions and across environments. There was no significant difference between the Familiar and CFC VR on Day 1. Licking behavior was collected only in a subset of mice (circle, n=5).

**(D-E)** The amount of freezing **(D)** and time taken to complete a lap **(E)** were not significantly different between the Familiar and CFC VR before fear conditioning (n=18). While not significantly different, there was a trend towards longer time taken in the first lap of the CFC VR, which we have observed before when mice enter novel environments from familiar ones[4]. The boxplots (in A, C-E) range from the first quartile (25th percentile) to the third quartile (75th percentile), and the box shows the interquartile range (IQR). The line across the box represents the median (50th percentile). The whiskers extend to 1.5*IQR on either side of the box, and anything above this range is defined as an outlier. P-values were calculated using a paired *t-test*.

The following day (Stage 3), mice were placed in the same VR environment with the tail- coat, but the water reward was removed (**Figure 1B**). Mice that continued to run at least three laps per minute with the tail-coat and without water reward advanced to the experiment stage (Stage 4). Around 40% of the mice dropped out at this stage. High levels of lap running during training were crucial to ensure mice were undeterred by both the tail-coat and the reward removal[10][38]. Our criteria for consistent running behavior with minimal pauses throughout these three stages of training ensured that any baseline freezing behavior was minimal, similar to freely moving animals, and allowed us to attribute freezing after CFC to fear conditioning. In summary, our criteria for selecting mice for the experimental stage of contextual fear conditioning required them to run consistently (>3 laps per minute) with 1) rewards, then 2) with a tail-coat, and then 3) without rewards plus the tail-coat. This threshold resulted in about 40% of the mice proceeding to the experimental stage. Once mice qualified for the experimental stage, they were no longer excluded from analysis due to their behavior. We tested three variations of the head-fixed CFC paradigm. In Paradigm 1, the neutral environment was the training VR environment, and a new VR environment was paired with shocks. In Paradigms 2 and 3, both the neutral and shock-paired environments were new and distinct from the training environment to better control for environmental familiarity. In Paradigms 1 and 2, the tail-coat was removed on the days following CFC, whereas in Paradigm 3, it remained on the mouse on all post-CFC days. With these paradigms, we varied some parameters that may influence fear memory recall, contextual discrimination, fear extinction, and their associated behaviors in head-fixed VR-based CFC paradigms. We detail these variations in the following sections, starting with Paradigm 1.

### When tested for contextual fear memory recall, mice displayed increased freezing behavior in the shocked-paired VR environment

On Day 0 of the experimental stage in Paradigm 1 (CFC day), mice (n = 18) were exposed to the same VR environment we used for training, referred to as the Familiar VR from here onwards (**Figure 1C**), for 10 minutes. We then switched them to a new VR environment (CFC VR). Following baseline exploration of the CFC VR for 10 minutes, we repeatedly applied mild-electric shocks (4-12 shocks, 0.5-1mA in amplitude, 1s long) to the mouse's tail. We call the period when shocks were delivered "during CFC". Shocks were pseudo-randomly administered with respect to the animal's position in the CFC VR, with an inter-shock interval (ISI) of 1 minute. To ensure that the shocks were associated with the context and not a specific position in the environment, no visual cues were explicitly paired with the shock. We quantified

the animal's response to the shocks and observed an immediate increase in running speed following each shock (**Supplementary Figure 1B**). This was consistent across all mice and shocks and was a reliable indicator that the apparatus was working correctly. Sixty seconds after the last shock was administered, the VR screens were switched off, the tail-coat was removed, and mice were returned to their home cages. The next day (Fear memory recall, Day 1), we tested for recall of the learned association between the VR environment and the fearful stimulus. Mice were exposed to both VRs (familiar VR and CFC VR) for five minutes each in a counterbalanced manner. Water reward remained absent on recall days; however, in this paradigm, the tail-coat was no longer present.

Before fear conditioning, mice exhibited similar behavior in both the Familiar and CFC VRs. We evaluated the time taken to complete a lap and the freezing behavior (defined as time points when the animal's instantaneous velocity dropped below 1cm/s). Neither metric revealed a significant difference between the two VRs before shock administration (**Figure 2A, Supplementary Figure 1D-E**). However, after CFC, when the animals were reintroduced to the VRs on recall Day 1, we observed a significant increase in freezing and time taken to complete a lap in the CFC VR compared to the Familiar VR (**Figure 2A-D**). As soon as mice transitioned to the CFC VR (either from dark or after the Familiar VR) on the recall day, we observed behaviors such as slowing down, freezing, moving backward, and hesitation to move forward (**Supplementary Videos 1-2**). This response was markedly different from their behavior in the Familiar VR. This difference in behavior can be observed clearly in most mice on the very first lap (**Figure 2A-B**). Since we removed the reward, we didn't find licking behavior to be indicative of recall behavior (**Supplementary Figure 1C**). However, some mice displayed licking behavior in the Familiar VR on Day 0 before fear conditioning, which was absent on Day 1. This is likely because mice had previously received a water reward in the Familiar VR. We will address this caveat in Paradigms 2 and 3.
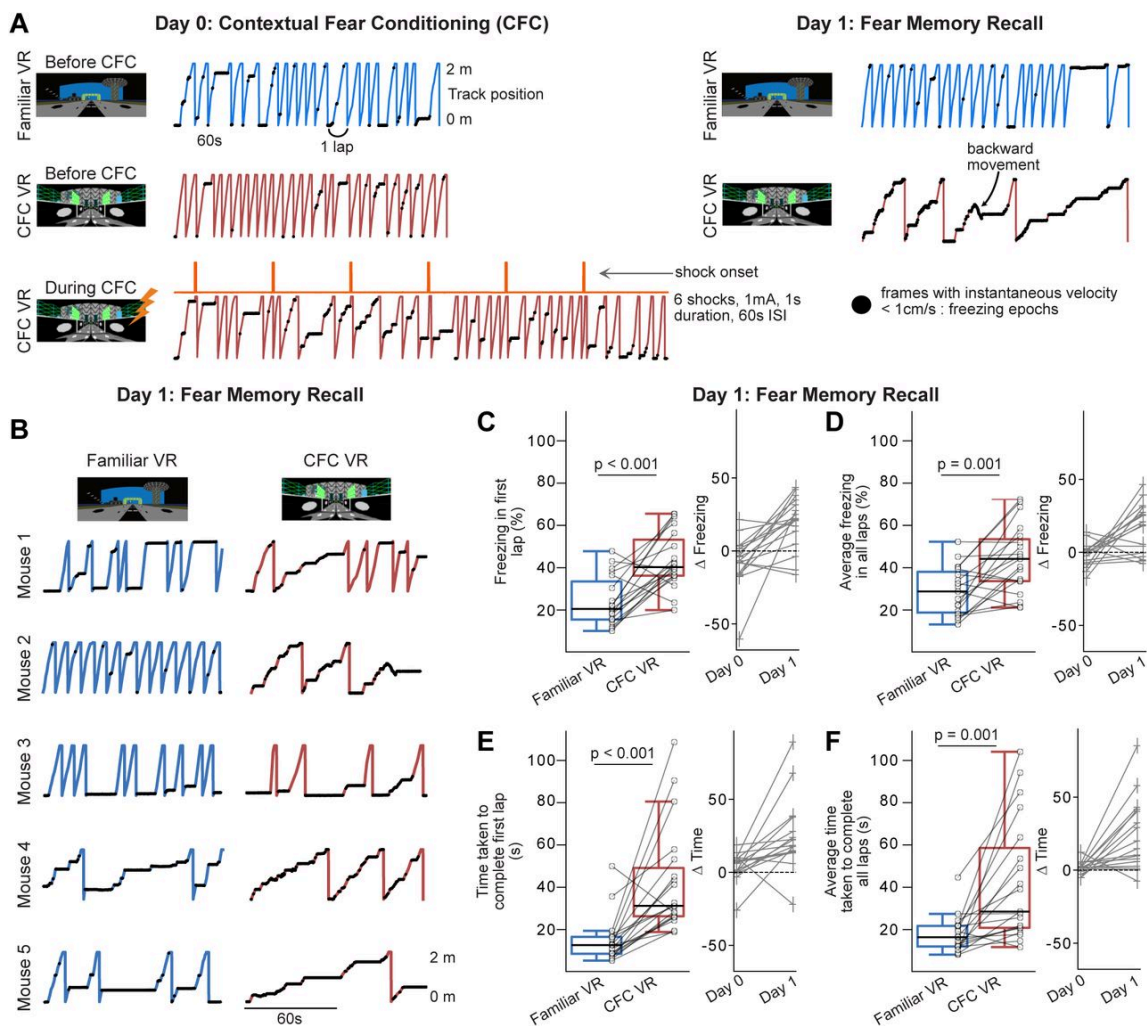
**Figure 2. Head-fixed mice show increased freezing behavior following contextual fear conditioning in the CFC VR.**

**(A)** A single example mouse's lap running behavior on experiment days, Day 0 and Day 1. Behavior is shown for approximately 3 minutes in all sessions except during CFC, which is shown for the 6 minutes that the session lasted. Frames where freezing was detected (instantaneous velocity <1cm/s) are marked with black dots. The traces on the right show that this mouse increased freezing, decreased velocity, and moved backward in the CFC VR (red traces) but not in the Familiar VR (blue traces) on Recall Day. This mouse received six shocks at 1mA intensity at 60 s inter-stimulus interval (ISI).

**(B)** First two minutes of recall behavior in more mice (n = 5) in Familiar VR versus CFC VR.

**(C-D)** (Left Average freezing percentage on recall day in the very first lap **(C)** and all laps **(D)** during the 5 minutes that mice explored the Familiar (blue) and CFC (red) VR. Freezing (%) was calculated as the number of frames where freezing was detected in a lap divided by the total number of frames in each lap. (Right) Delta calculated as the difference in the amount of freezing in the CFC VR compared to the Familiar VR before CFC (Day 0) and after CFC (Day 1). The dashed line represents 0.

**(E-F)** Same as C-D but for the time taken to complete the first lap **(E)** and all laps **(F).** Mice displayed an increase in freezing and in time taken to complete a lap in the first lap and, on average, in the CFC VR. In C-F, circles and pluses represent individual mice (n = 18, 16 male and two female mice). In C-F, data was pooled from mice receiving different numbers of shocks (4, 6, 12) at varying intensities (0.5 mA, 0.8 mA, 1 mA, and 1.2 mA), which is separately displayed in **Supplementary Figure 2**. Lines join data from the same mouse. P-values were calculated using a *paired t-test*.
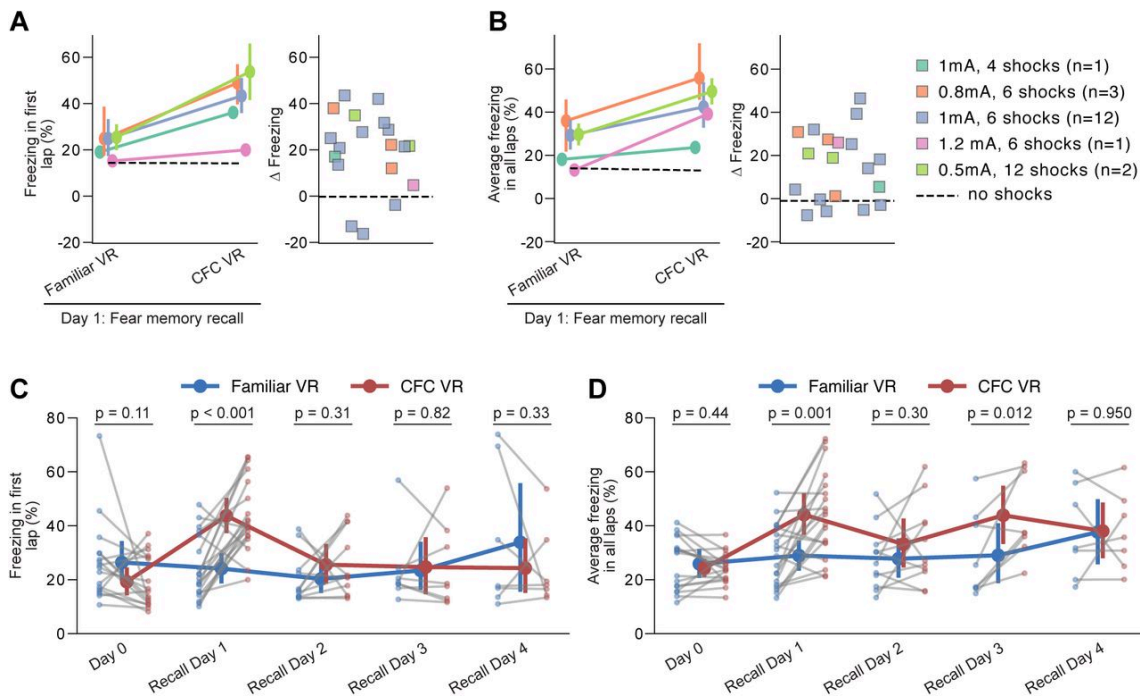
**Supplementary Figure 2. Change in freezing with shock amplitude, number of shocks, and across recall days.**

**(A-B)** The left panel shows the average freezing in the first lap **(A)** and all laps **(B)**. The right panel illustrates delta freezing, calculated as the difference in freezing between the CFC VR and the Familiar VR. The x-axis on the right panel is meaningless. A random jitter parameter separates the data points in the x-axis to prevent them from overlapping. The dashed line represents the average freezing percentage in a control paradigm, where mice experienced the same conditions without shocks. The largest effect sizes were observed in the first lap when the mouse received 0.5 mA, 12 shocks (lime green), or 0.8 mA/1 mA, 6 shocks (orange, purple). Four shocks produced a small effect. Increasing the number of shocks (to 6 or 12) enhanced freezing in the CFC VR. However, increasing shock intensity only led to modest increases in average freezing, as seen with 1.2mA, six shocks (pink) compared to 1mA, six shocks (purple). Number of animals used is indicated in the figure legend.

**(C-D)** A subset of animals underwent multiple days of recall tests (n = 18 Day 0, n = 18 Recall Day 1, n = 11 Recall Day 2, n = 8, Recall Day 3, n = 7 Recall Day 4). VR environments were presented in a counterbalanced manner for 5 minutes each day. The increase in freezing in the CFC VR was highest on the first day, both in the first lap **(C)** and across all laps **(D)**. P-values were calculated using a paired *t-test*.

When we quantified the freezing behavior in mice, we found it to be, on average, high throughout the five minutes that mice spent in the CFC VR on recall Day 1 (**Figure 2C-D**, average freezing (%), mean ± 95%

Confidence Intervals (CI), Familiar VR: 28.95 ± 5.47, CFC VR: 44.13 ± 7.75, p=0.001, Paired *t*-test). We also observed a significant increase in freezing during the first lap in the CFC VR compared to the familiar VR (**Figure 2B-C**, average first lap freezing (%), Familiar VR: 24.13 ± 5.59, CFC VR: 43.71 ± 6.49, p<0.001, Paired *t*-test). This freezing behavior also translated to mice taking longer to complete a lap in the CFC VR compared to the Familiar VR, both in the first lap (average time taken to complete first lap (s), Familiar VR: 14.90 ± 5.27, CFC VR: 42.78 ± 12.17, p<0.001, Paired *t*-test) and on average (**Figure 2E-F**, the average time taken to complete all laps (s), Familiar VR: 17.58 ± 4.18, CFC VR: 42.92 ± 13.96, p=0.001, Paired *t*-test). The increase in freezing and time taken to complete a lap in the CFC VR compared to the Familiar VR was significantly higher on Day 1 than Day 0, indicating that it results from fear conditioning (**Figure 2C-F**, p<0.05, Paired *t*-test).

Based on studies in freely moving animals[16][17][39][40][41], we settled on an intensity of 1 mA and six shocks as a reasonable protocol, which we tested on a sizeable cohort of mice (n = 12). We found that freezing at this intensity and shock number was higher on average in the CFC VR; however, mice showed variability in their responses (**Supplementary Figure 2A-B**). The majority of mice (7/12) displayed appropriate memory recall (**Supplementary Figure 2A-B**), indicated by more freezing in the CFC VR compared to the Familiar VR (delta > 0), while 3/12 mice froze more in the Familiar VR (delta < 0), and 2/12 showed equal freezing levels in both VRs (delta ≈ 0). Such variability has been regularly documented in freely moving animals and may not be unique to the VR setup used here[42][43][44][45][40][46]. Next, in a small group of mice (n = 6), we investigated whether changing the number of shocks or the shock amplitude would affect the conditioned fear response (**Supplementary Figure 2A-B**). We found that most shock amplitudes and numbers of shocks increased freezing behavior on average in the CFC VR on recall day (**Supplementary Figure 2A-B**). The observed variability was within the same range as that of the larger cohort of mice we tested using the 1 mA, 6-shock protocol (**Supplementary Figure 2A-B**). A more detailed analysis with a larger sample size may be necessary to understand further how variations in shock parameters affect the conditioned response, as has been done in studies with freely moving animals[47][48][49][45][50].

Finally, we examined the extinction of this conditioned response (**Supplementary Figure 2C-D**). We placed the animals in both the Familiar and the CFC VR for five minutes over four days (Recall Days 1-4) in a counterbalanced manner and tested their recall behavior. Mice displayed the most substantial increase in freezing in the CFC VR on the first day of recall (**Supplementary Figure 2C-D**, Average freezing (%): Recall Day 1: Familiar VR: 28.95 ± 5.47, CFC VR: 44.13 ± 7.75). Freezing on the first lap in the

CFC VR was also most pronounced on Recall Day 1 (First lap freezing (%): Recall Day 1: Familiar VR: 24.13 ± 5.59, CFC VR: 43.71 ± 6.49). Both average (Familiar VR: 27.78 ± 7.86, CFC VR: 33.19 ± 10.22) and first lap freezing (Familiar VR: 20.30 ± 6.24, CFC VR: 25.56 ± 8.03) in the CFC VR decreased on the second day of recall compared to the first recall day, becoming similar to the Familiar VR. While first lap freezing remained similar between the Familiar and the CFC VR on subsequent Recall Days 3 and 4, we observed variability in the average freezing behavior. Average freezing increased significantly again on Recall Day 3 in the CFC VR (Average freezing (%): Recall Day 3: Familiar VR: 29.05 ± 13.32, CFC VR: 43.89 ± 13.10) and was high in both VRs on Recall Day 4 (Recall Day 4: Familiar VR: 37.66 ± 15.77, CFC VR: 38.04 ± 13.42).

To quantify freezing levels more precisely, baseline freezing on Day 0 was compared to recall-day freezing using a Linear Mixed Effects (LME) Model, with recall days as fixed effects and mouse as a random effect (**Tables 1–2**). In the CFC VR, mice froze significantly more on Recall Days 1, 3, and 4 compared to Day 0. By Recall Day 4, freezing levels were elevated in both the Familiar and CFC VRs relative to baseline (**Table 2**). On the other hand, first-lap freezing showed a significant increase only on Recall Day 1 in the CFC VR and remained similar to Day 0 on Recall Days 2–4 in both VRs (**Table 1**). This pattern suggests that freezing in the CFC VR peaks on the first recall day, with a strong conditioned fear response to the shock-paired VR observed on Recall Day 1. The marked difference in freezing behavior between the CFC VR and Familiar VR during the first lap diminishes after the first recall day. On the other hand, average freezing behavior becomes more variable in subsequent recall days, suggesting that complete fear extinction in Paradigm 1 may take longer than four days. The increase in freezing on Recall Day 4 in the Familiar VR may reflect either fear generalization or a response to the extended lack of reward in a previously rewarded environment. Further research is needed to determine the exact conditions required for complete fear extinction in this paradigm.

| VR | Recall Day 1 | Recall Day 2 | Recall Day 3 | Recall Day 4 |
|---|---|---|---|---|
| Familiar VR | -2.28 ± 4.69, p=0.62 | -6.36 ± 5.50, p=0.25 | -2.92 ± 6.13, p=0.63 | 7.76 ± 6.41, p=0.23 |
| CFC VR | 24.34 ± 3.94, p<0.001 | 5.88 ± 4.62, p=0.21 | 5.50 ± 5.16, p=0.29 | 5.39 ± 5.40, p=0.32 |

**Table 1.** LME summary (estimate ± standard error, p-value) for first lap freezing in Paradigm 1 with fixed effects (recall days, baseline: before CFC, Day 0) and random effect (mouse).

| VR | Recall Day 1 | Recall Day 2 | Recall Day 3 | Recall Day 4 |
|---|---|---|---|---|
| Familiar VR | 2.35 ± 2.82, p=0.41 | 1.14 ± 3.40, p=0.74 | 3.05 ± 3.83, p=0.43 | 13.29 ± 3.98, p=0.0019 |
| CFC VR | 19.5 ± 3.63, p<0.001 | 8.44 ± 4.33, p=0.06 | 18.29 ± 4.86, p=0.0006 | 12.85 ± 5.07, p=0.016 |

**Table 2.** LME summary (estimate ± standard error, p-value) for average freezing in Paradigm 1 with fixed effects (recall days, baseline: before CFC, Day 0) and random effect (mouse).

In summary, these results demonstrate that head-fixed mice can acquire fear associations in VR environments. Most mice displayed freezing as a conditioned response specifically to the shock-paired VR—behavior that mirrors that of freely moving animals after fear conditioning. However, complete fear extinction in this paradigm may require more than four days of testing.

## *A second paradigm where head-fixed mice discriminate between two novel VRs*

As previously mentioned, the incomplete extinction of licking behavior in the familiar VR before fear conditioning or the gradual increases in freezing behavior in the familiar VR during recall tests may indicate that mice still associate the VR with water rewards, which could be a caveat. Furthermore, in traditional CFC paradigms with freely moving mice, fear behavior has been assessed mainly by comparing two novel contexts, one associated with shocks and the other acting as a control. To address this, we tested another paradigm (Paradigm 2), using a novel VR instead of the familiar VR to act as the control (**Figure 3A**). One novel VR was assigned as the Control VR, and a second novel VR was assigned as the CFC VR, which would later become paired with the shocks. In this paradigm, we also added an extra habituation day to increase the animal's pre- exposure time to the novel VRs prior to conditioning (Day –1). Pre-exposure to the context before fear conditioning can enhance contextual fear, as seen in freely moving animals[51][16][17][21][52][53].
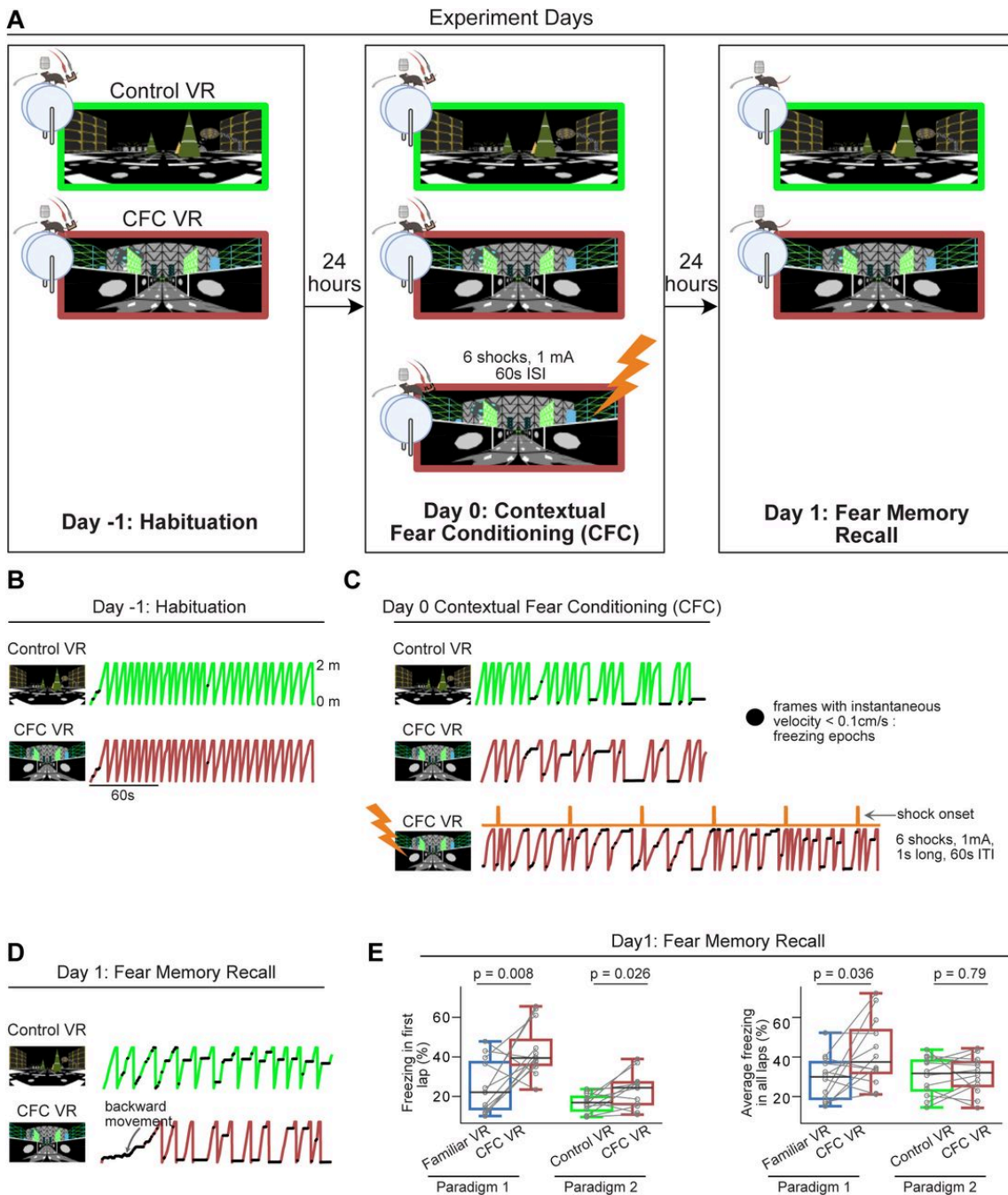
**Figure 3. Using a novel VR as the neutral environment instead of a familiar VR in a second paradigm results in modest increases in freezing.**

**(A)** The training paradigm is similar to paradigm 1. On experiment day, mice were introduced to two novel VRs, one of which would be associated with the shock (CFC VR) and the other wouldn't (Control VR). In this paradigm, there was an added habituation day, where mice were exposed to the two VRs for ten minutes. The next day, mice ran in the two VRs again before receiving mild electric shocks in the CFC VR. The recall test occurred the next day. In this cohort, all mice received six shocks at 1 mA intensity.

**(B-D)** These panels show the lap running behavior of a single mouse on experiment days 1, 2, and 3. Behavior

The training was done similarly to the previous paradigm. After mice showed consistent running behavior in the Familiar VR with the tail–coat and without reward, they were advanced to the experimental stage. On Day –1, mice were exposed to the two novel VRs for ten minutes each. On Day 0, they were re-exposed to the same two VRs for ten minutes before receiving six one–second-long mild electric shocks (at 1 mA and 1 minute ISI) in one of them - the CFC VR. On Day 1, mice were exposed to the two VRs for five minutes to evaluate memory recall (**Figure 3A-B**).

Compared to Paradigm 1, in the novel VRs, mice showed no differences in licking behavior across all experimental sessions (**Supplementary Figure 3A**). There was also no significant difference in freezing behavior and time taken to complete a lap between the two VRs on Day –1 and Day 0 before fear conditioning (**Supplementary Figure 3B–C**).
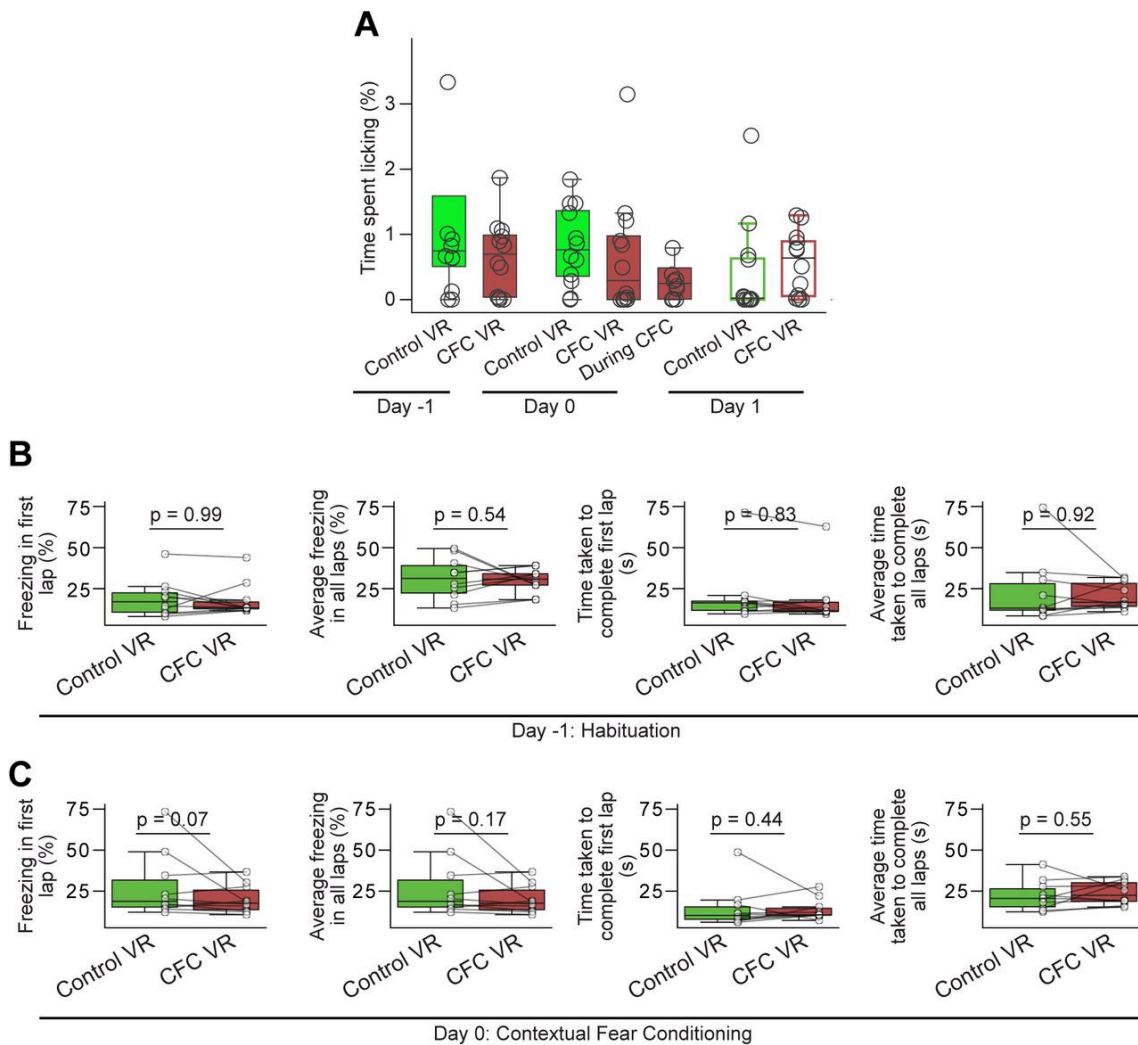
**Supplementary Figure 3. Licking and running behavior before fear conditioning, in Paradigm 2.**

**(A)** Licking behavior remains low in all sessions, unlike Paradigm 1. It does not significantly differ between the Control vs CFC VR before and after CFC.

**(B-C)** The amount of freezing and average running speed was not significantly different between the Control and CFC VR before fear conditioning, both on Day 1 **(B)** and Day 2 **(C)**. However, in this paradigm, some mice paused more on both days than in Paradigm 1. P-values were calculated using a *paired t-test*.

## *Head-fixed mice show heightened fear discrimination during the first lap when discriminating between two novel VRs*

We compared the freezing behavior between Paradigm 1 and Paradigm 2 on Recall Day 1 to the same intensity and number of shocks (1 mA, 1 s long, 60 s ISI, six shocks, n=12 mice each paradigm). We observed only modest increases in average freezing behavior and time taken to complete a lap in the CFC

VR in Paradigm 2, compared to Paradigm 1 (**Figure 3C-D, 4A-E**). The effect sizes for the difference in freezing behavior between CFC VR and Control VR in Paradigm 2 were smaller than those between Familiar VR and CFC VR in Paradigm 1 (Cohen's d: First lap freezing: Paradigm 1: 1.377, Paradigm 2: 0.917. Average Freezing: Paradigm 1: 0.893, Paradigm 2: 0.076). When we quantified freezing by lap on Recall Day 1 in Paradigm 2, we found that after the first lap, mice showed similar freezing in both the Control VR and the CFC VR across all subsequent laps (**Supplementary Figure 4**). In contrast, in Paradigm 1, mice consistently froze more in the CFC VR compared to the Familiar VR throughout Recall Day 1 (**Supplementary Figure 4**).
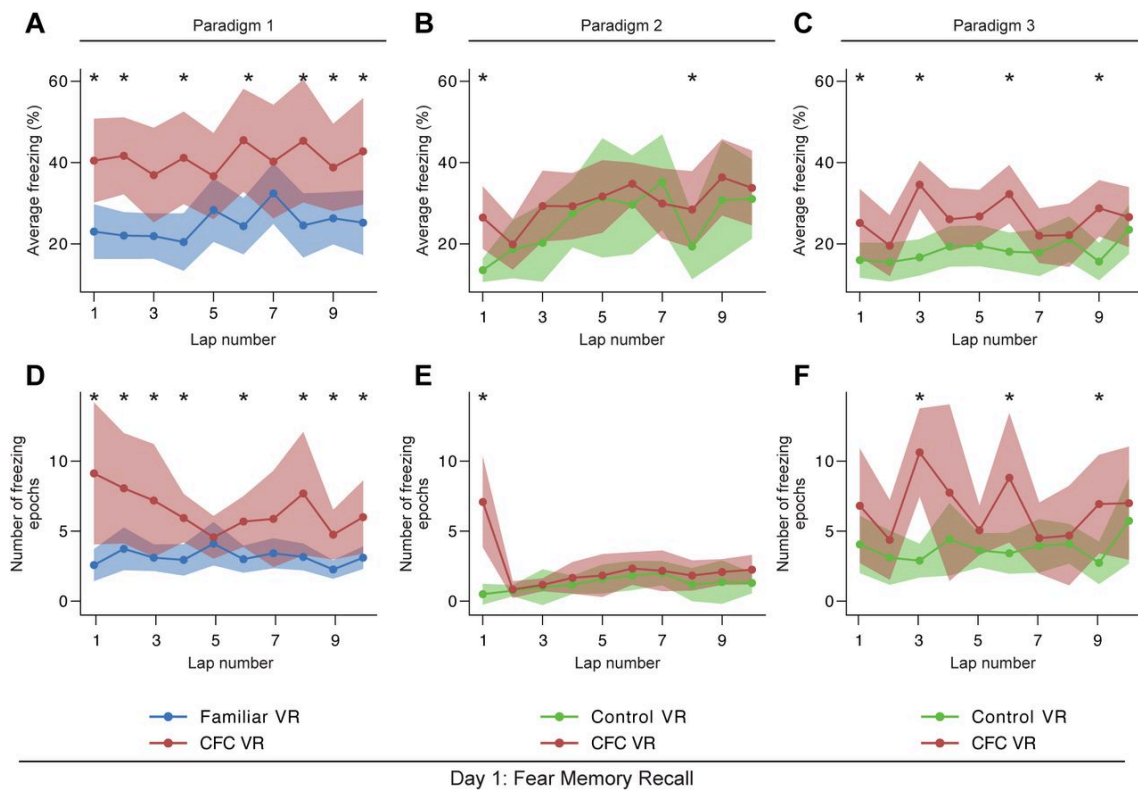


**Supplementary Figure 4. Lap-wise freezing behavior in the three paradigms.**

(**A–F**) Average freezing across mice (**A–C**) and the number of freezing epochs (**D–F,** see Methods) in each lap across the two VRs on the first day of recall in (**A, D**) Paradigm 1, (**B, E**) Paradigm 2 and (**C, F**) Paradigm 3. Lines indicate mean, and shading indicates 95% confidence intervals. P-values between (**A, D**) Familiar VR and CFC VR and (**B–C, E–F**) Control VR and CFC VR were calculated using a *paired t-test.* * indicates p–values<0.01.

Indeed, when we quantified freezing behavior in the Control VR and CFC VR in Paradigm 2, we found that the most significant increase in freezing in the CFC VR was observed in the first lap (freezing in first lap %: Control VR: 16.50 ± 3.15 CFC VR: 23.19 ± 5.75, p = 0.026, time taken to complete first lap (s): Control VR: 14.27 ± 2.85, CFC VR: 25.68 ± 5.55, p = 0.001, Paired *t*-test, **Figure 3**, **Figure 4A–E**). Neither average freezing (**Figure 4C**, average freezing in all laps %: Control VR: 30.32 ± 6.25, CFC VR: 31.06 ± 6.07, p=0.792, Paired *t*–test) nor time taken to complete all laps (**Figure 4E**, the average time taken to complete all laps: Control VR: 21.73 ± 8.11, CFC VR: 24.27 ± 6.36, p=0.558, Paired *t*-test) showed significant differences between the two VRs.
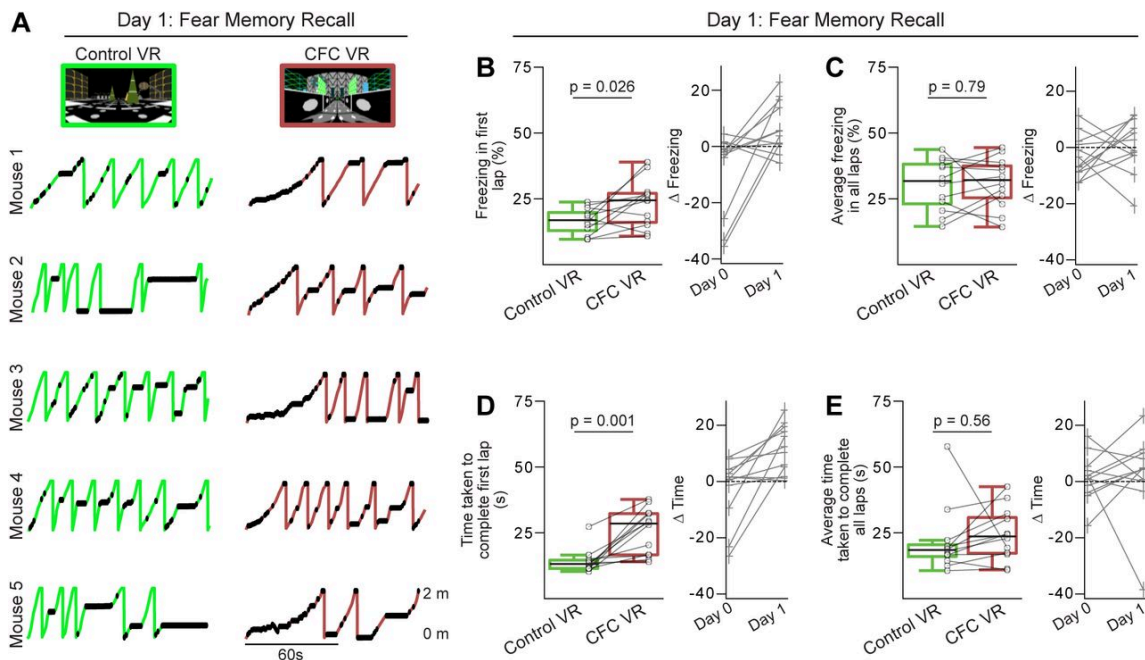


**Figure 4. In Paradigm 2, the most significant freezing and reduced speed occurred in the first lap of the CFC VR compared to the Control VR.**

**(A)** First two minutes of recall behavior in five mice in Control VR (green) versus CFC VR (red).

**(B–C)** The left panels show the amount of freezing on the recall day in (B) the very first lap and (C) all laps during the 5 minutes when the mice explored the Control (green) and CFC (red) VR. Freezing (%) is calculated as the number of frames where freezing was detected in a lap divided by the total number of frames in each lap. On the right, the delta is calculated as the difference in the amount of freezing in the CFC VR compared to the Control VR before (Day 2) and after CFC (Day 3). The dashed line represents 0.

**(D–E)** Same as B–C but for the time taken to complete the first lap **(D)** and all laps **(E).** In B–E, circles and pluses represent individual mice (n = 12). Lines join data from the same mouse. P-values were calculated using a *paired t-test.*

When mice were returned to the two VRs the following day for a second day of recall (Recall Day 2), we found no significant difference in first lap freezing between the Control and CFC VR (**Supplementary Figure 5**, First lap freezing (%) Recall Day 2: Control VR: 13.96 ± 4.24, CFC VR: 21.34 ± 6.79, p = 0.083, Paired *t*-test). Average freezing in both CFC VR and Control VR returned to baseline levels on Recall Day 1 and remained so on Recall Day 2 (**Supplementary Figure 5**, **Tables 3–4**, Average freezing (%) Recall Day 1: Control VR: 30.32 ± 6.25, CFC VR: 31.06 ± 6.07, p = 0.792, Recall Day 2: Control VR: 33.35 ± 6.11, CFC VR: 35.88 ± 5.89, p = 0.045, Paired *t*-test). This indicates that fear extinction in Paradigm 2 happens quickly, within the first recall session after the first lap.
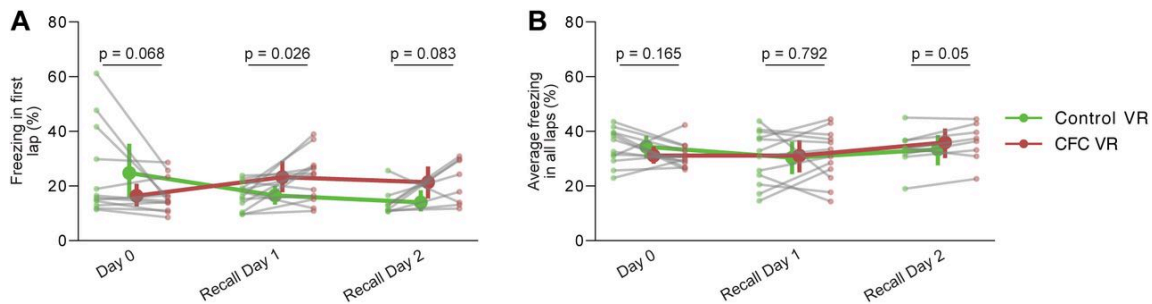


**Supplementary Figure 5. Mice extinguished their fear on the second recall day in Paradigm 2.**

**(A-B)** First lap freezing (A) and average freezing across all laps (B) across two days of recall in Paradigm 2. P-values were calculated using a paired t-test. Circles indicate data from individual mice (n = 12 for Recall Day 1 and n = 8 for Recall Day 2). Mice showed no significant difference in freezing behavior between the two environments on Recall Day 2.

| VR | Recall Day 1 | Recall Day 2 |
|---|---|---|
| Control VR | –8.22 ± 4.48, p=0.08 | –10.76 ± 5.01, p=0.05 |
| CFC VR | 6.82 ± 2.85, p=0.03 | 4.91 ± 3.24, p=0.15 |

**Table 3.** LME summary (estimate ± standard error, p-value) for first lap freezing in Paradigm 2 with fixed effects (recall days, baseline: before CFC, Day 0) and random effect (mouse).

| VR | Recall Day 1 | Recall Day 2 |
|---|---|---|
| Control VR | –3.99 ± 2.97, p=0.20 | –1.47 ± 3.37, p=0.67 |
| CFC VR | –0.02 ± 2.8, p=0.99 | 4.31 ± 3.17, p=0.19 |

**Table 4.** LME summary (estimate ± standard error, p-value) for average freezing in Paradigm 2 with fixed effects (recall days, baseline: before CFC, Day 0) and random effect (mouse).

## *A shorter ISI and leaving the tail-coat on during fear memory recall improved fear discrimination when using two novel VRs*

Freezing behavior in the CFC VR in Paradigm 2 was weaker than in Paradigm 1, with rapid fear extinction after the first recall lap. In Paradigm 3, two parameters were changed relative to Paradigm 2 to test whether freezing behavior and fear discrimination could be enhanced. First, the interval between consecutive shocks was reduced to see if a shorter ISI could produce a more robust fear response[54][55]. Second, the tail-coat was kept on during memory recall, based on evidence that removing contextual cues can reduce conditioned freezing (González et al., 2003). We hypothesized that the tail-coat might act as a contextual cue and that its presence during recall might enhance freezing behavior.

In Paradigm 3, mice followed the same experimental protocol as Paradigm 2, with two novel VRs: one assigned as the Control VR and the other as the CFC VR. A habituation day in the two new VRs (Day –1) was followed by the CFC day (Day 0), where mice received six shocks (0.6 mA, 20-26 s ISI) in the CFC VR. This was followed by recall days (Days 1-3), where mice explored the two VRs presented in a counter-balanced manner. Unlike the other two paradigms, in Paradigm 3, the tail-coat remained on during the recall days (**Figure 5A**).
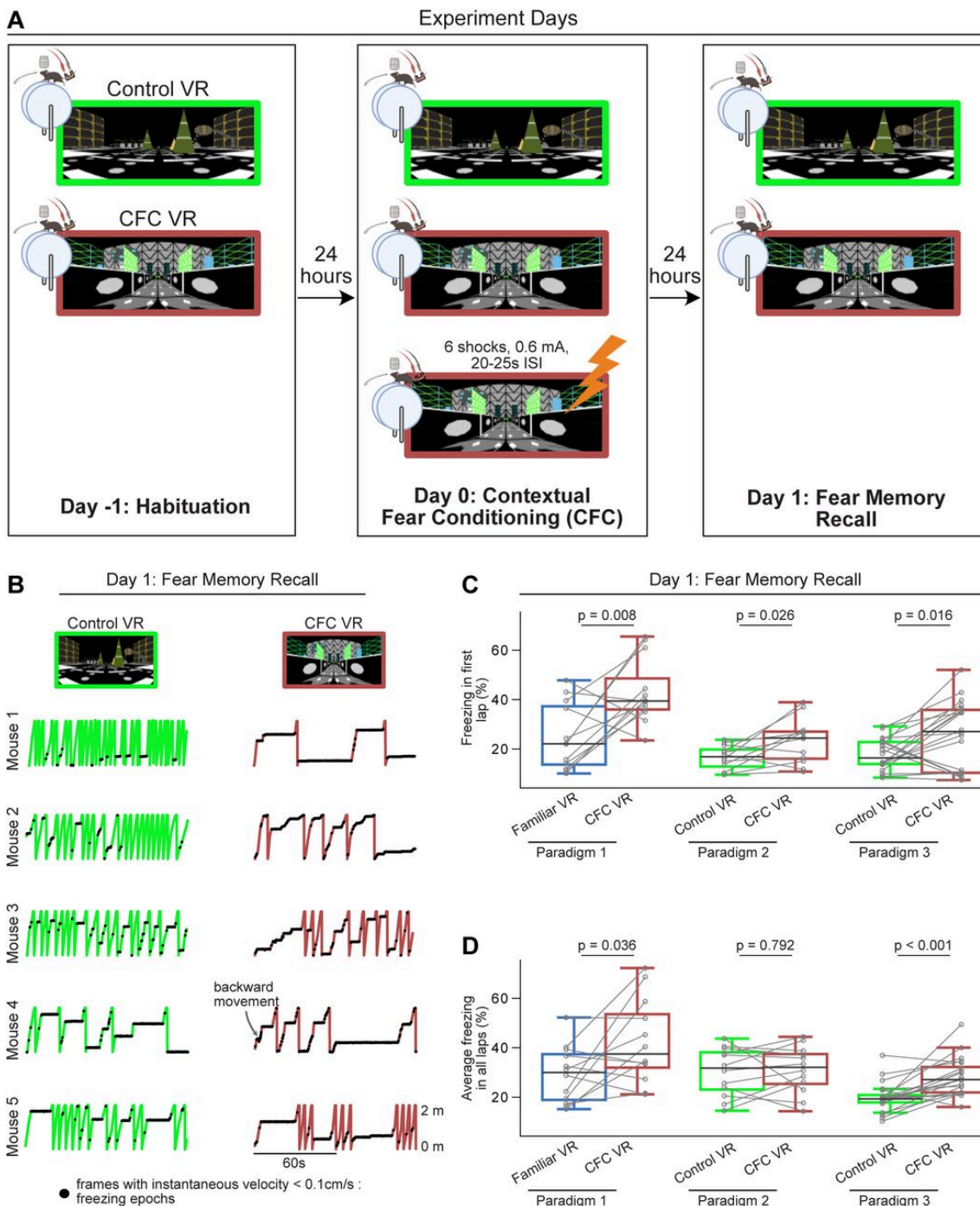
Figure 5. A third paradigm that uses a novel VR as the neutral environment but keeps the tail-coat on during memory recall led to increased freezing in the CFC Environment.

(A) The training and experiment paradigm was similar to Paradigm 2 except that the shocks were administered closer together (20-25 s ISI), and the tail-coat was kept on during recall days.

(B) First two minutes of recall behavior in Paradigm 3 in five mice in Control VR (green) versus CFC VR (red).

(C–D) Comparison between freezing in the first lap (C) and all laps (D) in paradigm 1 (blue and red) versus paradigms 2 and 3 (green and red). n = 12 mice were used in paradigms 1 and 2 (10 male and two female mice),

and n = 20 mice in paradigm 3. P-values were calculated using a *paired t-test*. In Paradigm 3, by keeping the tail-coat on during the recall days, we observed an increase in freezing in the CFC VR in the first lap and across all laps compared to Paradigm 2.

We found that mice (n = 20) showed better fear discrimination between the Control and CFC VRs in Paradigm 3 compared to Paradigm 2 (**Figure 5B–D**). Mice not only showed more significant freezing in the first lap (freezing in first lap %: Control VR: 17.83 ± 2.95 CFC VR: 25.86 ± 6.51, p = 0.016, Paired *t*-test) but average freezing across all laps was also higher in the CFC VR compared to the Control VR (**Figure 5C–D**, **Figure 6A–D**, average freezing in all laps %: Control VR: 19.86 ± 2.87, CFC VR: 28.19 ± 3.66, p < 0.001, Paired *t*-test).
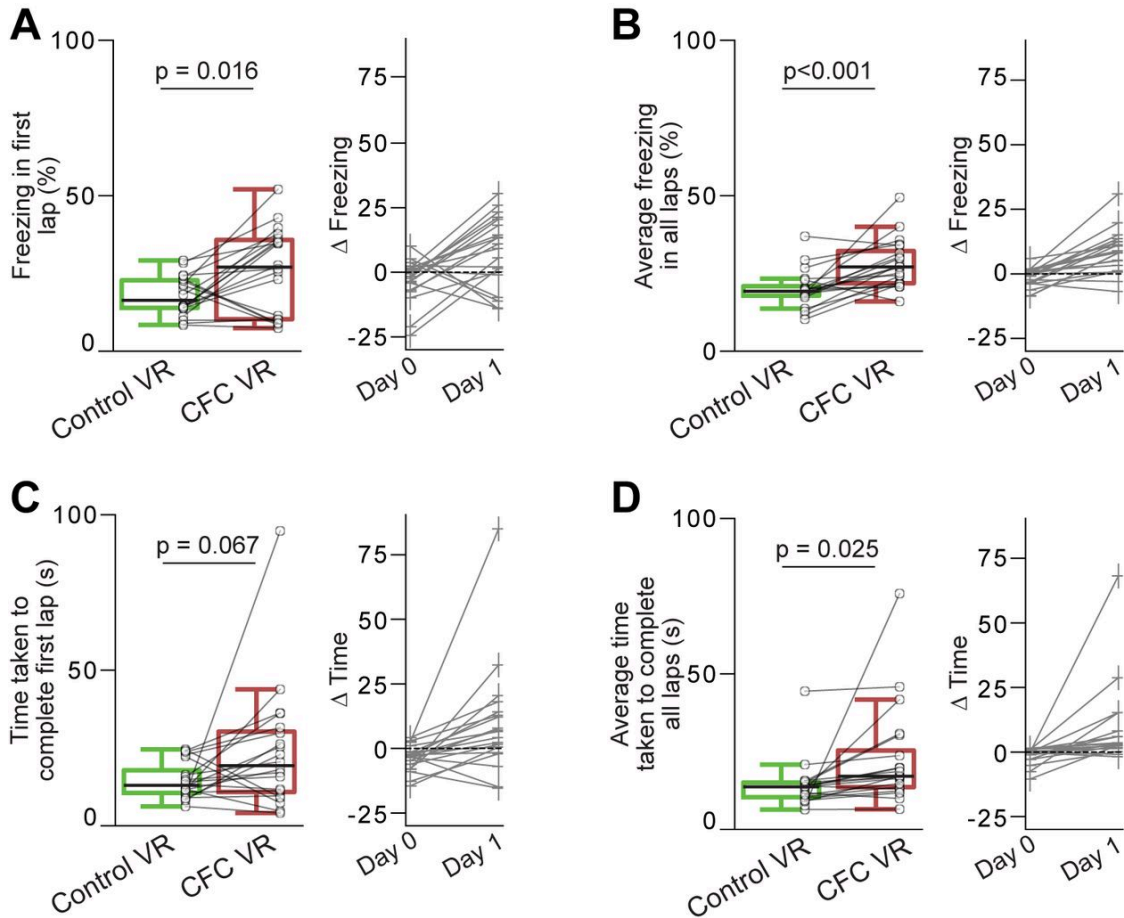
**Figure 6. Mice froze more and reduced speed in Paradigm 3 across all laps on Recall Day 1; this freezing behavior continued into the second day of recall in Paradigm 3.**

**(A-B)** The right panels show the amount of freezing on the recall day in **(A)** the very first lap and **(B)** all laps during the 5 minutes when the mice explored the Control (green) and CFC (red) VR. Freezing (%) is calculated as the number of frames where freezing was detected in a lap divided by the total number of frames in each lap. On the left, the delta is calculated as the difference in the amount of freezing in the CFC VR compared to the Control VR before (Day 2) and after CFC (Day 3). The dashed line represents 0.

**(C-D)** Same as A-B but for time taken to complete the first lap **(C)** and all laps **(D).** Circles and pluses represent individual mice (n = 20). Lines join data from the same mouse. P-values were calculated using a *paired t-test.*

While first-lap freezing showed a weaker effect size in Paradigm 3 compared to the other paradigms, there was a strong effect of average freezing across the session (Cohen's d: First lap freezing: Paradigm 1: 1.377, Paradigm 2: 0.917, Paradigm 3: 0.744. Average Freezing: Paradigm 1: 0.893, Paradigm 2: 0.076, Paradigm 3: 1.185). On average, we found that Paradigm 1 still produced the highest absolute freezing

behavior in the CFC VR (average freezing in all laps %: CFC VR: Paradigm 1: 44.13 ± 7.75, Paradigm 2: 31.06 ± 6.07, Paradigm 3: 28.19 ± 3.66). The difference in freezing behavior between the CFC VR and the neutral VR was greatest in Paradigm 1 ($\Delta$ average freezing (CFC VR − Familiar/Control VR): Paradigm 1: 13.14, Paradigm 2: 0.74, Paradigm 3: 8.33). However, unlike Paradigm 2, where the largest differences in freezing between the CFC VR and the Control VR were restricted to the first lap, the shorter ISIs and the addition of the tail- coat during the recall day in Paradigm 3 improved contextual fear discrimination between the two novel VRs. When tested for memory recall in Paradigm 3, mice froze more in the CFC VR than in the Control VR, and this effect persisted beyond the first lap (**Figure 5C-D, Supplementary Figure 4**).

Additionally, unlike the rapid fear extinction seen in Paradigm 2, mice showed a delay in extinction in Paradigm 3 (**Table 5-6**, **Supplementary Figure 6**). Average freezing continued to be higher in the CFC VR than in the Control VR on Recall Day 2 (Average freezing (%) Recall Day 1: Control VR: 19.86 ± 2.87, CFC VR: 28.19 ± 3.66, $p < 0.001$, Recall Day 2: Control VR: 21.79 ± 3.70, CFC VR: 26.46 ± 3.34, $p < 0.001$, Paired *t*-test). By Recall Day 3, there was no significant difference in freezing between the Control VR and the CFC VR (First lap freezing (%): Recall Day 3: Control VR: 13.10 ± 3.37, CFC VR: 17.37 ± 5.15, $p = 0.151$, Average freezing (%): Recall Day 3: Control VR: 19.43 ± 3.18, CFC VR: 20.73 ± 3.61, $p = 0.240$, Paired *t*-test).
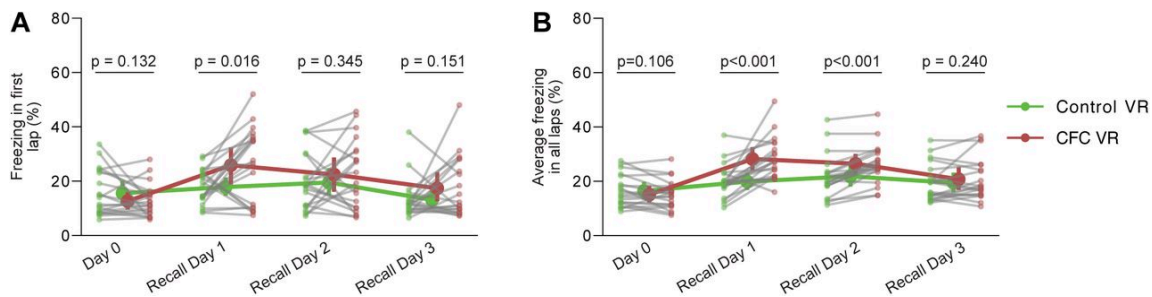


**Supplementary Figure 6. Mice show delay in extinction in Paradigm 3.**

**(A-B)** Freezing in the first lap **(A)**, and average freezing across all laps **(B)** in the Control VR vs CFC VR on three consecutive recall days in Paradigm 3. The tail-coat was kept on all recall days. P-values were calculated using a *paired t-test*.

| VR | Recall Day 1 | Recall Day 2 | Recall Day 3 |
|---|---|---|---|
| Control VR | 2.29 ± 2.51, p=0.37 | 3.96 ± 2.51, p=0.12 | –2.43 ± 2.51, p=0.34 |
| CFC VR | 13.21 ± 3.33, p<0.001 | 9.79 ± 3.34, p=0.005 | 4.73 ± 3.34, p=0.16 |

**Table 5.** LME summary (estimate ± standard error, p-value) for first lap freezing in Paradigm 3 with fixed effects (recall days, baseline: before CFC, Day 0) and random effect (mouse).

However, when comparing average freezing to baseline levels on Day 0 using an LME model, a significant increase in average freezing was observed in both the Control VR and CFC VR groups. This increase persisted across all three recall days (**Tables 5-6**). Unlike Paradigm 1, in Paradigm 3, freezing levels showed a downward trend over time. However, like Paradigm 1, they had not returned to baseline by the third recall day, suggesting that fear was not entirely extinguished. The presence of the tail-coat during recall days likely contributed to some degree of fear generalization, as mice showed elevated freezing relative to baseline even in the Control VR. However, freezing levels in the Control VR remained much lower than in the CFC VR on all days, indicating that mice continued to discriminate between the VR environments (**Figure 6, Supplementary Figure 6**, **Tables 5-6**).

| VR | Recall Day 1 | Recall Day 2 | Recall Day 3 |
|---|---|---|---|
| Control VR | 3.43 ± 1.28, p=0.01 | 5.35 ± 1.28, p=0.0001 | 2.99 ± 1.28, p=0.02 |
| CFC VR | 13.15 ± 1.78, p<0.001 | 11.42 ± 1.78, p<0.001 | 5.69 ± 1.78, p=0.0023 |

**Table 6.** LME summary (estimate ± standard error, p-value) for average freezing in Paradigm 3 with fixed effects (recall days, baseline: before CFC, Day 0) and random effect (mouse).

There was no difference in first-lap freezing in the Control VR compared to baseline on any of the recall days. First-lap freezing in the CFC VR was still higher than baseline on Recall Day 2; however, it was back to baseline levels by Recall Day 3 (**Table 5-6**). As we noticed in Paradigm 1, this indicates that pronounced

increases in freezing in the CFC VR in the very first lap are most prominent in the earlier days of recall. On the other hand, the increases in average freezing continue to persist and may take longer to extinguish. Thus, a shorter ISI and the presence of the tail-coat during memory recall may enhance conditioned fear in head-fixed mice when discriminating between two novel VRs. The influence of each parameter on its own will need further investigation.

In summary, our results show that mice exhibited greater average freezing behavior in the CFC VR in Paradigms 1 and 3 compared to Paradigm 2. In Paradigm 2, the most noticeable increase in freezing occurred during the very first lap in the CFC VR compared to the Control VR. We found that fear discrimination could be improved with a shorter ISI when presenting tail shocks and when the tail-coat was present during memory recall, as shown in Paradigm 3. Furthermore, in Paradigms 1 and 3, the fear was not wholly extinguished over the days we tested for recall and may take longer. However, fear extinction was rapid in Paradigm 2 and was back to baseline levels within the first day of recall. Thus, we provide three different variations for performing CFC in head-fixed mice that can be used to understand the neural underpinnings of fear memory.

## *Place cells in the CA1 subregion of the hippocampus displayed remapping and decreased field widths following contextual fear conditioning*

The hippocampus plays a critical role in the encoding, consolidation, and recall of memories and is necessary for the expression of contextual fear memory[22][56][57][21][31][58][59][53]. Context is thought to be represented in the hippocampus by place cells that fire at specific spatial locations (place fields) in an environment[60]. These place cells have been thought to help discriminate between feared and neutral contexts. Previous studies on freely moving animals have shown that fear conditioning can cause place cells to remap[61][62][63][64][65][66][67][68][69][70]. Remapping is defined by place cells shifting their firing fields, indicative of place cells adapting to incorporate new information into memory[71][72][73]. Additionally, a recent study[67] that performed calcium imaging of hippocampal cells in freely moving mice found that fear conditioning narrows the width of place fields in the feared environment. This suggests that place cells encode the same environment on a finer scale following fear conditioning, potentially enhancing context discrimination and threat avoidance[67].

We replicated these findings in our head-fixed version of CFC in VR. To investigate the effect of fear conditioning on place cell activity in our task, we expressed a calcium indicator, GCaMP6f[74], in

hippocampal pyramidal cells and, using two- photon microscopy, imaged from the same hippocampal neurons across days during fear conditioning and fear memory recall in Paradigm 1 (**Figure 7A-B**). We found that a subset of place cells formed before CFC remained stable, while others remapped or changed their preferred firing locations after CFC (see examples in **Figure 7C, 7D–G**). This is similar to previously reported observations[61][65][68][69].
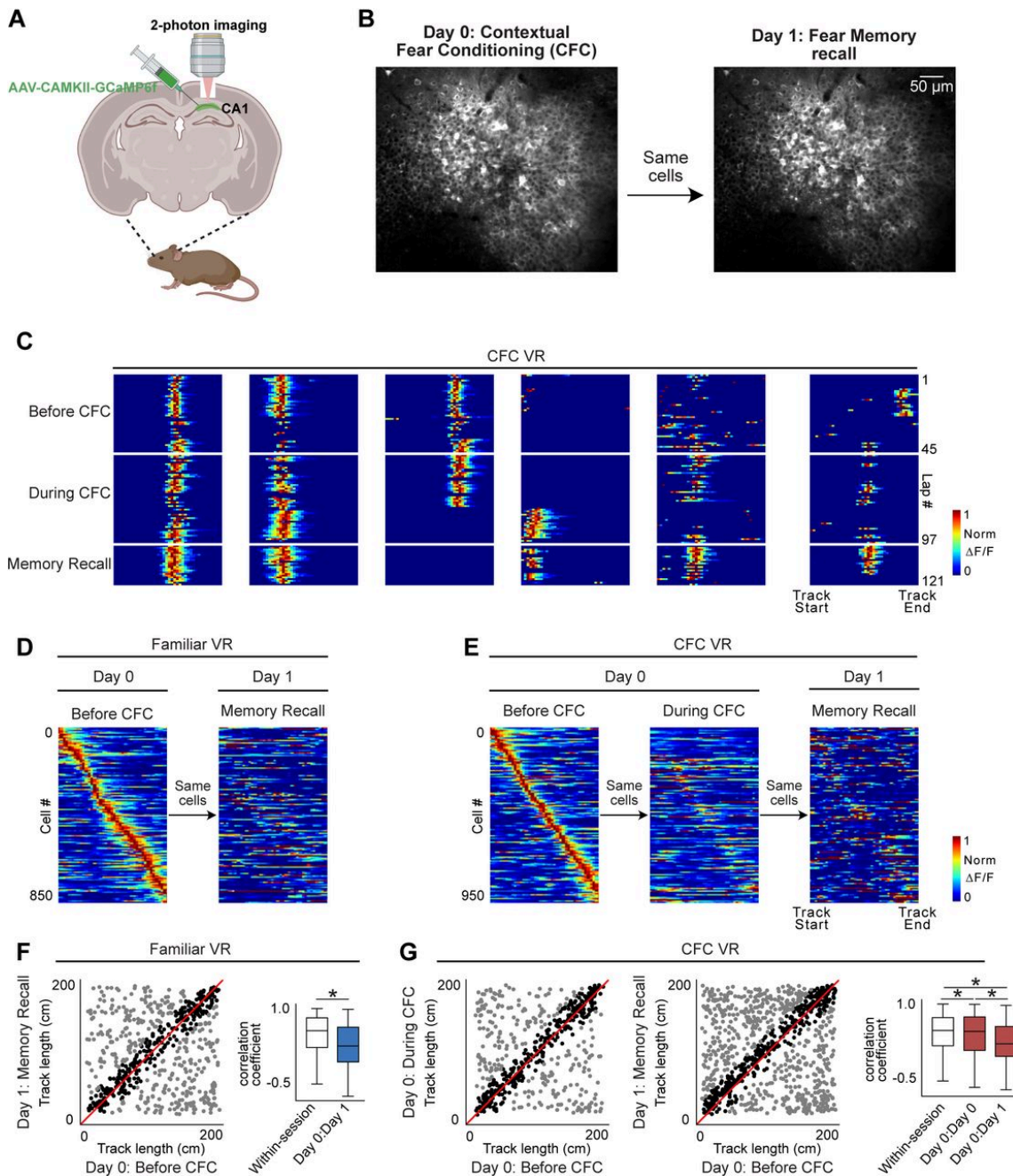
**Figure 7. Fear conditioning results in place cell remapping in both Familiar and CFC VR.**

**(A)** A schematic of the procedure for two-photon imaging of large populations of the same CA1 neurons over multiple days, created with BioRender.com

**(B)** An example field of view across the two experiment days. The same field of view was aligned and imaged across days.

**(C)** Examples of a few place cells in the CFC VR across sessions on Day 0 (before CFC, during CFC) and Day 1 (Memory Recall). White lines separate laps in each session. Some place cells maintain stable fields across days, while others remap.

**(D)** Place fields defined on Day 0 in Familiar VR before CFC are plotted across Day 1 during fear memory recall (n = 4 mice).

**(E)** Place fields defined on Day 0 in CFC VR before CFC are plotted across the fear conditioning session and on Day 1 during fear memory recall.

**(F)** On the left is a scatter plot of the center of mass of place fields defined in Familiar VR before CFC on Day 0 (x-axis) compared to their center of mass on Day 1 during fear memory recall (y-axis). On the right is a boxplot of correlation coefficients between mean place fields defined in Familiar VR before CFC on Day 0 and memory recall on Day 1 (Day 0: Day 1). The within- session correlation coefficients serve as control and were calculated between mean place fields in the first half and second half of the Familiar VR before the CFC session.

**(G)** A scatter plot of the center of mass of place fields defined in CFC VR before CFC on Day 0 (x-axis) compared to their center of mass on (right) Day 0 during CFC and (middle) Day 1 during memory recall. On the left is a distribution of correlation coefficients between mean place fields defined in Familiar VR before CFC on Day 0 and during CFC (Day 0: Day 0) and memory recall on Day 1 (Day 0: Day 1). The within-session correlation was calculated between mean place fields in the first half and second half of the CFC VR before the fear conditioning session. Asterisk (*) indicates significant $P$ values (KS test, $P < 0.01$). Our findings show that place fields present in the before CFC sessions in both Familiar and CFC VR showed significant remapping following fear conditioning.

We found remapping to occur in both the Familiar and the CFC VR to similar extents, as indicated by the lower correlation across sessions/days compared to the within-session correlation (**Figure 7F–G**). This contradicts previous findings by Moita et al.[65], who reported more stability in the control environment compared to the CFC environment after fear conditioning. This remapping in both the Familiar and the CFC VR could be due to differences in the CFC paradigm used in that study versus ours and will need further investigation. It could also result from taking the water reward away from a previously rewarded VR, as is the case in Paradigm 1. We have shown before that this makes the place map more likely to drift across days[10][38]. Whether these results hold the same for the Control VR in Paradigms 2 and 3 will need further investigation.

Next, we looked at the place cells in each session. Interestingly, we found an increase in the number of place cells in the CFC VR during memory recall, a finding not previously reported (**Figure 8A–B**). We also found that place cells had narrower fields in the CFC VR during memory recall (**Figure 8C**), as previously shown[67]. We did not find a significant difference in other place cell parameters we examined, such as

lap–by–lap reliability (**Figure 8D**) and out-of-field firing (**Figure 8E**). Thus, our observations of remapping and narrower place field widths replicate findings from freely moving animals, validating our paradigm's use to explore further questions using the head-fixed preparation to study the neural underpinnings of contextual fear memories. We add to this field by showing an increase in the proportion of place cells following CFC, a possible neural substrate of fear memory recall.
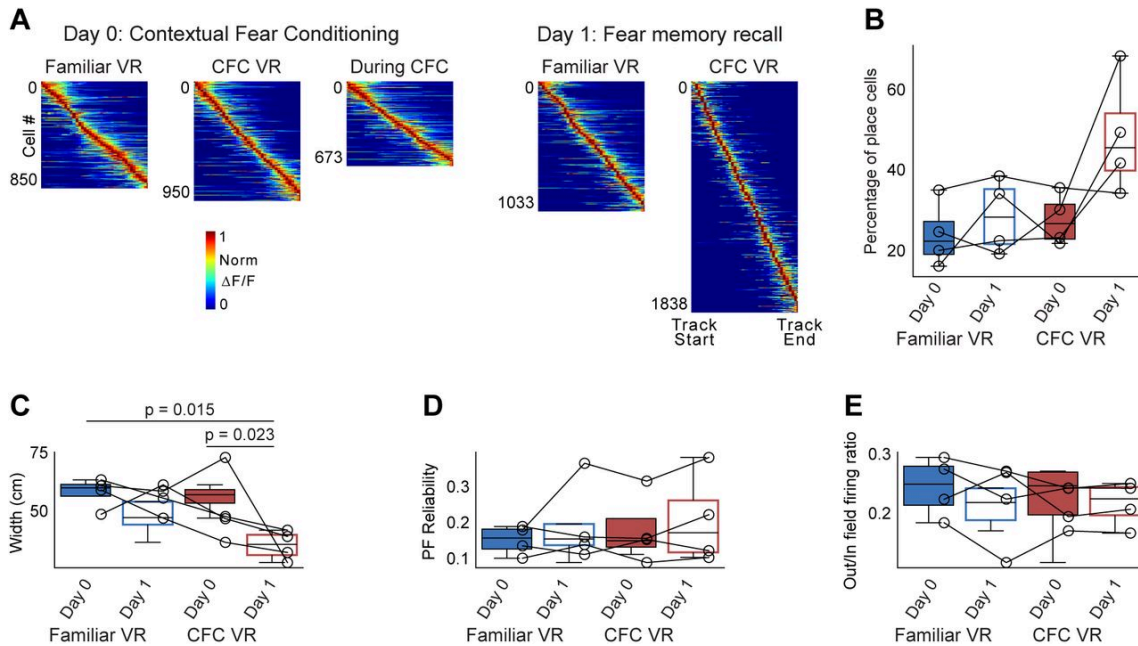


**Figure 8. The widths of place fields in CA1 narrow during memory recall.**

**(A)** Place fields were defined and sorted by track length in each session, pooled from all mice (*n* = 4 mice). Each cell's activity was normalized to its peak, and cells were sorted by their center of mass along the track.

**(B)** The percentage of place cells is calculated as the number of place cells divided by the total number of recorded cells. More place cells were identified by our algorithm in the CFC VR on Day 1.

**(C-E)** Parameters of place fields: **(C)** Width, **(D)** Place Field (PF) Reliability, and **(E)** out/in field firing ratio in both VRs on Day 0 and Day 1. The width of the place fields in the CFC VR significantly decreased on Day 1. No other parameters significantly varied across days. P-values were calculated using a *paired t-test*.

# Discussion

We present three paradigms for performing CFC in head-fixed mice, using a conductive "tail–coat" to deliver aversive shocks as mice navigate VR environments on a treadmill.

Our key findings are: 1) Head-fixed mice exhibited freezing behavior in response to an aversive stimulus in VR, consistent with conditioned responses seen in freely moving animals. Freezing was especially pronounced during the first lap in the fear-conditioned environment compared to the neutral environment across all paradigms tested. 2) With mice on a spherical treadmill, additional conditioned responses such as hesitation and backward movement were detected. 3) The choice of neutral environment influenced fear discrimination: mice froze more in the fear-conditioned VR when the neutral environment was familiar rather than novel. Freezing in the fear-conditioned VR could be enhanced by shorter ISIs and the presence of the tail-coat during recall when the neutral environment was novel. 4) Following fear conditioning, place cells in the hippocampal CA1 region showed remapping, increased numbers, and narrower fields, paralleling findings in freely moving animals and offering new insights.

Here, we experimented with three paradigms for fear conditioning in mice, with the main difference being the neutral environment where the mice didn't receive any shock. In Paradigm 1, the neutral VR was familiar, where the mice had previously received rewards, and the CFC VR was novel. In Paradigms 2 and 3, both the neutral and CFC VRs were similarly novel. In Paradigm 3, we decreased the ISI and kept the tail-coat on the animal when testing for memory recall. Thus, we have tested three different variations for performing CFC in head-fixed mice. On average, mice showed more freezing behavior in the CFC VR compared to the neutral VR. A common feature across all paradigms was pronounced freezing during the very first lap in the CFC VR. While mice in Paradigm 2 extinguished fear rapidly after the first lap, freezing behavior persisted up to 3-4 recall days in Paradigms 1 and 3, to varying degrees. We also observed variability in conditioned responses across mice. Some displayed an opposite pattern, freezing more in the neutral VR or equally in both VRs. This variability in behavior, similar to that observed in freely moving animals[42][43][44][45][40][46], can be insightful when combined with investigations of neural activity, helping to understand the neural dynamics that contribute to an animal's ability to learn the association between a context and fearful stimuli. This can reveal the mechanisms by which such memories may generalize or become maladaptive, as seen in post-traumatic stress disorders.

We have shown here an example of using Paradigm 1 to study place cells in the hippocampus and their role in fear memory formation and recall. We recorded from a large group of the same hippocampal CA1 cells across days and demonstrated that place cells remap and narrow their place field widths with fear conditioning. This occurs in head- fixed mice navigating VR environments, similar to freely moving animals. Narrow place fields may suggest sharper spatial tuning to incorporate a salient emotional

memory and may aid in context discrimination[67]. However, how place cells narrow their widths in response to fear conditioning remains an open question. One possible way to answer this is by imaging CA1 place cell dendrites to understand how they integrate inputs before and after fear conditioning. We can explore what dendritic firing and plasticity mechanisms lead to narrow place field widths. We can then perturb these firing patterns to attribute causality to the narrowing of place field widths in fear discrimination. Our head-fixed paradigm enables the recording of dendrites and the study of plasticity mechanisms[75][12], thus facilitating these investigations.

We recently used Paradigm 3 to understand the role of the thalamic nucleus reuniens- hippocampal pathway[37]. Using a two-photon microscope, we identified neural activity in this pathway by imaging axons from the nucleus reuniens that project to the CA1 with single-axon resolution. We found this pathway necessary for suppressing fear memory retrieval, context discrimination, and fear extinction. The robust freezing response in Paradigm 3 in the fear-conditioned VR, compared to a neutral novel VR, allowed us to align our findings with the existing literature on the role of the nucleus reuniens- hippocampal circuit in fear memory in freely moving animals[76][39][77][78][79][80]. Furthermore, the subcellular resolution achieved through two-photon calcium imaging using the head-fixed preparation allowed us to longitudinally observe and understand the inputs that axons from the reuniens send to the hippocampus during fear memory formation and retrieval, a level of detail that is difficult to achieve with current techniques in freely moving preparations.

In another unpublished study, we used Paradigm 2 and identified co-active neurons between CA1 and CA3 subregions of the hippocampus during fear memory recall. The difference between the first and subsequent laps has helped us understand the progression of neural activity in the hippocampus as mice go from retrieving the fear memory to extinction within one session. Moreover, the variability in response across mice has allowed us to regress the neural activity to the behavior, identifying neural differences between those mice that accurately recall the fear memory and those that do not. These studies showcase the broad applicability of our different CFC paradigms.

In the laboratory, CFC provokes freezing behavior in freely moving rodents, as demonstrated by several studies that span decades[16][17][27][20][21][58][81]. In our study, we found that a mild electric shock applied to the tail could also trigger freezing behavior as the conditioned response in head-fixed mice, making our paradigm more comparable to the freely moving paradigms than previously attempted methods using air-puff stimulation[33][34]. There are numerous future opportunities to test how various parameters, such as shock amplitude, number of shocks, duration of fear conditioning, the configuration

of the Control versus CFC VR, or adding more sensory cues, may influence the animal's recall and extinction behavior and how it is encoded in the brain[17][82][56][83][45]. Moreover, our technique enables us to conduct a more detailed analysis of the animal's behavior. For example, besides freezing behavior, we have observed a sprinting behavior or a 'flight response' in response to each shock delivery and instances of fear-related backward movements during memory recall; defensive behaviors that have also been observed in freely moving animals[42][84][46][41]. As our mice are head-fixed, our setup allows easy measure of pupil diameter, respiration, vocalization, heart rate, and body temperature. These have been shown to change with fear conditioning[85][86][87][88][89].

There are also opportunities to use machine-learning-empowered algorithms to parse out new behavior markers for contextual fear memory, such as gestures or facial expressions[90][91][92][93]. Thus, we can understand the animal's behavior in a well-controlled environment, which when combined with neural activity recording, can lead to new insights into the neural circuits mediating different defensive responses and emotional states.

Significant insights into memory mechanisms through the CFC task have also come from recent discoveries of memory engrams in the brain[94][95][57][96]. Engram cells, identified in various brain regions with the help of genetic tagging and optogenetics, play a crucial role in encoding, consolidating, and retrieving specific memories. Typically, these cells are identified based on the expression of the immediate early gene *Fos* during fear conditioning. Their artificial activation with optogenetics can trigger memory recall, evidenced by increased freezing behavior. Understanding which neurons form these engram cells, how *Fos* expression is driven during memory formation, how memory information is stored in these cells, how they evolve with learning, and how their activation results in memory recall is an active area of research[97][98][99][100][101][102]. Incorporating our paradigm with simultaneous measurements of cellular and subcellular activity can help answer some of these questions. For instance, a recent study[99] tagged engram cells during fear conditioning while animals were freely moving and then imaged the spontaneous dynamics of these cells using two- photon imaging before and after fear conditioning. The study revealed that cells forming engrams were inherently more active. A limitation of this study was the separate contexts for imaging versus tagging, which can be addressed with our paradigm. Our CFC paradigm allows for direct neural recording of these cells before, during, and after tagging in the same context to examine how activity during memory formation relates to engram cell emergence, population dynamics, and memory recall. Furthermore, holographic stimulation techniques can reactivate specific cell ensembles of interest to help understand the causal relationships between

engram cells and memory. Moreover, the hippocampus contains both place cells and engram cells, both of which appear to be involved in contextual memory. However, their relationship is not yet fully understood. Our CFC paradigm offers an opportunity to study both place cells, as we have shown here, and engram cells simultaneously. This can be achieved by incorporating techniques that allow for *in vivo* labeling of *Fos*[100]. Thus, our head-fixed version of the CFC paradigm opens new avenues for research into the neural underpinnings of fear learning and memory.

Another advantage of our method is that it allows for studying changes in neuronal dynamics in response to an aversive stimulus, such as a shock. Our fields of view during the shock and subsequent flight-like response periods remained stable, and we could correct image movements during these periods with Suite2p[103]. This is a significant improvement over one-photon and electrophysiological techniques, where abrupt movements such as those induced by an electric shock can change fields of view and reduce the likelihood of recording from the same groups of cells, thereby hindering longitudinal assessments of neural dynamics. In Paradigm 1, where we imaged hippocampal cells during shock, we did not find cells responding to the shock itself, as others have reported[104][98][101]. We suspect this could be due to the number or duration of shocks administered and our shocks not being associated with a specific cue or location. In future studies, we plan to optimize these parameters to understand better how neural dynamics change in response to an aversive cue.

Finally, we recognize that our head-fixed CFC paradigm has some limitations. Compared to the freely moving CFC, our setup is less naturalistic. We defined different contexts as two visually distinct VR environments while odor, sound, and tactile cues remained constant. This could have made it harder for mice to differentiate between the two contexts, particularly in Paradigm 2. Unlike freely moving animals in CFC studies, our mice were water-restricted throughout the experimental process. Because the animals need to get used to wearing a tailcoat and running in the VRs without a reward, we tend to 'over-train' the mice. This criterion excludes mice that are less adept at running, limiting the number that go through the process and requiring larger cohorts of mice. Furthermore, despite our best efforts to include equal numbers of male and female mice, only some female mice reached the experimental stage. We believe this is due to the tail-coat weight and the reduced weight of females after water restriction compared to males (see Methods). Although we observed no behavioral differences between the four tested females and the male mice, we cannot guarantee similar results in other female animals without further testing. Studies indicate that different sexes may display varying conditioned responses, as seen in rats[105][106]. In the future, we aim to address these limitations.

In conclusion, we have developed a head-fixed version of the classic CFC paradigm. Our findings demonstrate that mice exhibit freezing behavior when fear-conditioned in a VR environment. Moreover, we observed that hippocampal place cells remap and narrow their fields in response to fear conditioning, mirroring observations in freely moving animals. This innovative paradigm bridges the behavioral task gap for techniques requiring head-fixation, paving the way for new investigations into neural circuits and deepening our understanding of the neural foundations of emotional memory.

# Methods

## Subjects

All experimental and surgical procedures adhered to the University of Chicago Animal Care and Use Committee guidelines. This study utilized 10-12 week-old C57BL/6J and Tg(Grik4-cre) G32-4Stl/J mice. Following the start of water restriction, the mice were individually housed in a reverse 12-hour light/dark cycle, and behavioral experiments were conducted during the animals' dark cycle.

## Head-fixation surgery

Mice were anesthetized with 1-2% isoflurane and given an intraperitoneal injection of 0.5 mL of saline and a subcutaneous injection of 0.45 mL of Meloxicam (1-2 mg/kg). A small incision was made on the skull to attach a metal head-plate (9.1 mm x 31.7 mm, Atlas Tool and Die Works) to head-restrain the mice. Some mice also had an imaging window implanted above the hippocampus, as previously described[4][10][12]. Post-surgery mice were housed individually. After a recovery day, they were water-restricted to 0.8-1.0 ml/day.

## Behavior training

Head-restrained mice were trained to run on a spherical treadmill to navigate virtual reality (VR) environments similar to the setups previously described[4][10][12]. Behavioral training began seven days following the water restriction. Briefly, VR environments were created using the Virtual Reality MATLAB Engine, or VIRMEN[107], and projected to five screens covering the mouse's field of view. Mice were head restrained with their limbs resting on a freely rotating Styrofoam wheel, which acted as a treadmill. VR environments were 2 m linear tracks. Mice received a water reward (4 µl) through a waterspout upon completing each traversal of the linear track, considered a lap. This reward was followed by a 1.5- second

pause in the VR to allow the mouse to consume the water. The mice were then virtually teleported to the start of the track to begin a new lap. Training sessions lasted 30 minutes per day. Mice were considered well-trained when they could run at >3 laps per minute. We found that this level of training was necessary to ensure that mice would continue to run even without rewards[10][38]. Generally, about 60% of mice met our criteria, which typically took around 10-14 days to achieve. Behavior data was collected using a PicoScope Oscilloscope (PICO4824, Pico Technology, v6.13.2).

## Tail-coat

A custom-designed "tail-coat" delivered mild electric shocks to a head-fixed mouse's tail during virtual reality (VR) navigation. A pictorial representation of the tail-coat can be found in **Figure 1D**. The tail-coat, handmade from wearable conductive fabrics, featured a lightweight design to ensure the mouse could continue running during baseline VR exploration (**Table 7**). First, the mouse's tail was measured while anesthetized for head- plate surgeries. A small denim patch cloth (Michael's) was cut into a rectangle to fit snugly on the mouse's tail. Marks were made where snap buttons (Michael's) would be sewn, ensuring they clipped just above the tail. Given that the mouse's tail narrows away from the body, the buttons closer to the body were placed slightly further apart than those closer to the tip. Typically, the buttons were set 2 cm apart on the narrow end and 2.5 cm apart on the broader end. Care was taken to adjust the placement of the buttons so they weren't too tight or loose for the mouse. We found that these measurements were generally similar across sexes and for the age group that we tested. After measurements were taken and the cloth cut, small strips of 8mm wide conductive fabric tape (Adafruit) were attached to either side of the cloth, with some tape hanging off the edge. A metal strip (McMaster Carr) of the same width was affixed to this portion of the tape to provide a secure grip for alligator clips used in fear conditioning. Finally, snap buttons were sewn with conductive thread at the marked spots. Clear nail polish was applied to secure the threads in place. The tail-coat creation process should take less than half an hour. Dimensions of the cloth for a typical male mouse, 12 weeks of age and weighing ~30 g, are shown in **Figure 1D**. The denim cloth was 4 cm in width and 3.2 cm in length; the conductive tape was 1.2 cm in width and 5.2 cm in length, with 1.5 cm hanging out at each side.

| Item | Manufacturer | Link |
|---|---|---|
| Denim patch cloth | Any fabric or hobby shop | https://www.michaels.com/product/loops-threads-denim-patches-assorted-10113795 |
| Snap Buttons | Any fabric or hobby shop | https://www.michaels.com/product/loops-threads-sew-on-snaps-10354228?michaelsStore=1191&inv=14 |
| Conductive nylon fabric tape | Adafruit | https://www.adafruit.com/product/3960 |
| Stainless conductive thread – 3 Ply | Adafruit | https://www.adafruit.com/product/641 |
| Multipurpose 304 Stainless steel sheet | McMaster-Carr | https://www.mcmaster.com/products/304-stainless-steel/multipurpose-304-stainless-steel-6/?s=304-stainless-steel |
| Shock box | Colbourn precision animal shocker | https://lafayetteinstrument.com |
|  | Alternate: Lafayette Instruments Scrambled Grid Current Generator |  |

**Table 7.** Items required to for head-fixed contextual fear discrimination

## Contextual fear conditioning protocol in head-fixed mice

Once the mice were well-trained and met our criteria of running >3 laps per minute, they were ready for the next stage. The following day, a tail-coat was attached to the mouse's tail. Mice that maintained consistent running in the VR, with minimal pauses, while wearing the tail-coat advanced to the next stage. For mice startled by the tail-coat, we typically attempted another day with the tail-coat, rewarding them and observing if their running behavior improved to running at least three laps per minute. If not, these mice were not advanced to the next stage. In mice that do advance, on the subsequent day, the tail-

coat was kept on, and the water reward was removed. All else remained the same, including the 1.5 s pause at the end, since we wanted animals to be able to distinguish the start and end of a lap. If the mice continued to run as before, they moved on to the experiment stage. From that day forward, the mice no longer received water reinforcement when running in the VR environments. Typically, about 40% of mice made it to the experiment stage. Tail-coats were only added during VR exploration and removed before returning the animals to their home cage. Once the mice advanced to the experiment stage, they were taken through the entire process and not excluded from analysis, even if they showed signs of inconsistent running behavior, which happened with some mice (for instance, see **Supplementary Figure 3B-C**).

We implemented three distinct paradigms to assess contextual fear discrimination. In the first paradigm, we conducted experiments over two days (Paradigm 1). On Day 0, mice engaged with the same VR in which they were trained, now referred to as the Familiar VR. After 10 minutes, we transitioned them to a new VR for another 10 minutes; this new VR would later be associated with shocks (CFC VR). During this phase, the mice explored both VRs without any rewards while wearing the tail-coat. After the initial exploration in the CFC VR, they received six mild electric shocks, each lasting 1 second with 1-minute intervals in between. The shocks were administered using a shock generator (Colbourn Precision animal shocker, Harvard Bioscience). A TTL pulse was generated using custom-written codes in MATLAB to turn on the shock generator via an Arduino. The shock times were recorded by the PicoScope Oscilloscope (PICO4824, Pico Technology, v6.13.2). We tested different shock intensities ranging from 0.5 to 1.2 mA. After the last shock, mice were removed from the VR and returned to their home cage. The following day (Day 1), we placed the mice in the Familiar VR or CFC VR for ten minutes to test their memory recall. No rewards were delivered during this phase; however, the tail-coat was not added during memory recall. Some mice underwent additional recall tests over subsequent days to assess the time required for fear memory extinction. As a control, some mice underwent the same paradigm but without any shocks.

In the second paradigm (Paradigm 2), the experiment spanned over three days. On Day – 1, mice explored two novel VRs for ten minutes each, establishing a baseline for context exploration. One of these VRs served as a control, while the other, the CFC VR, was where the mice would later receive electric shocks. On Day 0, the mice again spent ten minutes each in the Control and CFC VRs. After this, they received six mild electric shocks, each lasting one second, with a strength of 1 mA and an inter-trial interval of one minute. The mice wore the tail-coat on both Days –1 and 0. On Day 1, the mice were placed in either the Control VR or CFC VR for ten minutes each, in a counterbalanced manner, to test for memory recall. No

rewards were given on all the experimental days; however, the tail-coat was not added to the tails on the recall day (Day 1). The third paradigm (Paradigm 3) was similar to Paradigm 2 and used two novel VRs, except that a tail-coat was also added to the mice's tails during recall tests.

Additionally, a subset of mice in Paradigms 1 and 2 and all mice in Paradigm 3 went through multiple days of recall tests. The subset of mice was randomly chosen, not based on their recall behavior from the previous day. Mice were presented with either the CFC VR or the Control VR in a counterbalanced manner.

All VRs were randomly assigned as either Control or CFC VR to prevent biasing any inherent preferences in mice. However, the Familiar VR was always kept the same. We also used both sexes in our experiments. However, we found female mice less receptive to the "tail-coat" than their male counterparts. We believe this is due to the low average weight of female mice (~16 g) following water restriction. Female mice of the same age (10-12 weeks) weighed significantly less than males (20-23 g vs 25-30 g) and lost further weight following water restriction. As a result, only four female mice could proceed through and complete all the behavioral tests. Our ultimate goal is to compare behavior and neural activity across sexes, considering sex as a biological variable. To achieve this, we plan to adjust the age and use female mice of appropriate weight to ensure they can run on the treadmill with the tailcoat in the future.

## Behavior measurement

Freezing periods were periods during which the animal's instantaneous velocity was lower than 1 cm/s. Freezing epochs were defined as continuous, uninterrupted freezing periods longer than 1 s. The time taken to complete a lap was calculated as the total time (in seconds) the animal took to run from 0 to 200 cm.

## Surgery and two-photon imaging

Stereotaxic surgeries and cannula window implantation above the CA1 subregion of the hippocampus were performed in the same way as previously reported[10]. Briefly, a genetically-encoded calcium indicator, AAV1-CamKII-GCaMP6f (pENN.AAV.CamKII.GCaMP6f.WPRE.SV40 was a gift from James M. Wilson − Addgene viral prep #100834-AAV1; https://www.addgene.org/100834/; RRID: Addgene_100834) was injected (~50 nL at a depth of 1.25 mm below the surface of the dura) using a beveled glass micropipette leading to GCaMP6f expression in a large population of CA1 pyramidal cells. Mice underwent water restriction (1.0 ml/day) following viral injection and, seven days later, were implanted with a hippocampal window and head plate[3]. Mice were allowed to rest from the surgeries for 3-4 days,

after which behavioral training began. Imaging was done using a laser scanning two–photon microscope (Neurolabware). The setup is the same as the one previously described[10]. Time–series images were collected through Scanbox (v4.1, Neurolabware), and the PicoScope Oscilloscope (PICO4824, Pico Technology, v6.13.2) was used to synchronize frame acquisition timing with behavior. At the end of the imaging session on Day -1 or Day 0, a 1-minute time-series movie was collected at a higher magnification and then averaged to aid as a reference frame in finding the same imaging plane on subsequent days. Across-day images collected were motion-corrected using Suite2p[103] and aligned using ImageJ (v1.53, NIH). Region of interests were extracted using Suite2p.

## Place cell extraction and place field parameters

Place fields were identified as previously described[4][10]. Briefly, the 2 m track was divided into 40 position bins (each 5 cm wide). The running behavior of the animal was filtered to exclude periods where the animal was immobile (speed <1 cm/s). Filtering ensured that place cells were defined only during active exploration and not during freezing bouts. We have previously found that filtering versus not filtering yields similar results[10]. Extracted place fields satisfied the following criteria, which were used for all conditions and all mice: 1. The average ΔF/F was greater than 10% above the baseline. 2. The cell displayed significant calcium transients on >30% of laps in the field. 3. The rising phase of the mean transient was located on the track. 4. Their p-value from bootstrapping was <0.05. Multiple place fields within the same cell were treated independently. Parameters of place fields were calculated as described before[10]; this includes the center of mass (COM), place field reliability, out/in-field firing ratio, and place field widths.

## Statistics

For related samples, we performed a paired t-test. Multiple comparisons of related samples were corrected with Bonferroni post-hoc. To quantify freezing across days, we employed a linear mixed-effects model with days of recall as the fixed effect and behavior prior to fear conditioning on Day 0 as baseline. The model also included a random effect for mice to account for the nesting of observations within individual subjects. Separate models were used for each VR. Boxplots are plotted to display the entire distribution of the data. The box in the boxplot ranges from the first quartile (25th percentile) to the third quartile (75th percentile), and the box shows the interquartile range (IQR). The line across the box represents the median (50th percentile). The whiskers extend to 1.5*IQR on either side of the box,

and anything above this range is defined as an outlier. A two-tailed Kolmogorov–Smirnov (KS) Test was used to compare distributions. When not using boxplots, mean and confidence intervals are displayed.

## Notes

Supplementary videos can be downloaded from the following link:

https://uchicago.box.com/s/t1nkkadmv1bt6wa8ab3y32b5vel7x9x7

## Statements and Declarations

### Funding

### Author contributions

S.K. and M.S. conceived the idea. S.K. and M.S. supervised the project. S.K. designed the experiments. S.K., C.D., H.R., D.M., and C.C. collected the data. S.K. and C.D. analyzed the data. S.K., C.D., H.R., and M.S. interpreted the data. S.K. prepared the manuscript draft. All authors reviewed the results, provided feedback, and approved the final version of the manuscript.

### Conflicts of interest

The authors declare no competing interests.

### Data and code availability

Behavior data, imaging data, and scripts used for data analysis are available on GitHub at https://github.com/seethakris/CFCMethodspaper.

### Acknowledgments

## Footnotes

- https://uchicago.box.com/s/t1nkkadmv1bt6wa8ab3y32b5vel7x9x7

## References

1. ^*Bando Y, Wenzel M, Yuste R (2021). "Simultaneous two-photon imaging of action potentials and subthreshold inputs in vivo." Nature Communications. 12(1): 7229.*

2. ^*Chaigneau E, Ronzitti E, Gajowa MA, Soler-Llavina GJ, Tanese D, Brureau AYB, Papagiakoumou E, Zeng H, Emiliani V (2016). "Two-Photon Holographic Stimulation of ReaChR." Frontiers in Cellular Neuroscience. 10: 234.*

3. a, b, c*Dombeck DA, Harvey CD, Tian L, Looger LL, Tank DW (2010). "Functional imaging of hippocampal place cells at cellular resolution during virtual navigation." Nature Neuroscience. 13(11): 1433–1440.*

4. a, b, c, d, e, f, g*Dong C, Madar AD, Sheffield MEJ (2021). "Distinct place cell dynamics in CA1 and CA3 encode experience in new environments." Nature Communications. 12(1): 2977.*

5. ^*Emiliani V, Cohen AE, Deisseroth K, Hausser M (2015). "All-Optical Interrogation of Neural Circuits." Journal of Neuroscience. 35(41): 13917–13926.*

6. ^*Fan LZ, Kim DK, Jennings JH, Tian H, Wang PY, Ramakrishnan C, Randles S, Sun Y, Thadhani E, Kim YS, Quirin S, Giocomo L, Cohen AE, Deisseroth K (2023). "All-optical physiology resolves a synaptic basis for behavioral timescale plasticity." Cell. 186(3): 543–559.e19.*

7. ^*Hattori R, Komiyama T (2022). "Longitudinal two-photon calcium imaging with ultra-large cranial window for head-fixed mice." STAR Protocols. 3(2): 101343.*

8. ^*Heer CM, Sheffield MEJ (2024). "Distinct catecholaminergic pathways projecting to hippocampal CA1 transmit contrasting signals during navigation in familiar and novel environments." eLife. 13. doi:10.7554/eLife.95213.*

9. ^*Hernandez O, Papagiakoumou E, Tanese D, Fidelin K, Wyart C, Emiliani V (2016). "Three-dimensional spatiotemporal focusing of holographic patterns." Nature Communications. 7: 11928.*

10. a, b, c, d, e, f, g, h, i, j, k, l, m*Krishnan S, Heer C, Cherian C, Sheffield MEJ (2022). "Reward expectation extinction restructures and degrades CA1 spatial maps through loss of a dopaminergic reward proximity signal." Nature Communications. 13(1): 6662.*

11. ^Russell LE, Dalgleish HWP, Nutbrown R, Gauld OM, Herrmann D, Fişek M, Packer AM, Häusser M (2022). "All-optical interrogation of neural circuits in behaving mice." Nature Protocols. 17(7): 1579–1620.

12. a, b, c, d, eSheffield MEJ, Dombeck DA (2015). "Calcium transient prevalence across the dendritic arbour predicts place field properties." Nature. 517(7533): 200–204.

13. ^Guo ZV, Hires SA, Li N, O'Connor DH, Komiyama T, Ophir E, Huber D, Bonardi C, Morandell K, Gutnisky D, Peron S, Xu N-L, Cox J, Svoboda K (2014). "Procedures for behavioral experiments in head-fixed mice." PloS One. 9(2): e88678.

14. ^Juczewski K, Koussa JA, Kesner AJ, Lee JO, Lovinger DM (2020). "Stress and behavioral correlates in the head-fixed method: stress measurements, habituation dynamics, locomotion, and motor-skill learning in mice." Scientific Reports. 10(1): 12245.

15. a, bBouton ME (1993). "Context, time, and memory retrieval in the interference paradigms of Pavlovian learning." Psychological Bulletin. 114(1): 80–99.

16. a, b, c, d, eFanselow MS (1980). "Conditional and unconditional components of post-shock freezing." The Pavlovian Journal of Biological Science: Official Journal of the Pavlovian. 15(4): 177–182.

17. a, b, c, d, e, fFanselow MS (1990). "Factors governing one-trial contextual conditioning." Animal Learning & Behavior. 18(3): 264–270.

18. ^Kim JJ, Fanselow MS (1992). "Modality-specific retrograde amnesia of fear." Science. 256(5057): 675–677.

19. ^LeDoux JE (2000). "Emotion circuits in the brain." Annual Review of Neuroscience. 23: 155–184.

20. a, bMaren (2001). "Neurobiology of Pavlovian fear conditioning." Annual Review of Neuroscience. 24(1): 897–931.

21. a, b, c, d, eMaren, Phan KL, Liberzon I (2013). "The contextual brain: implications for fear conditioning, extinction and psychopathology." Nature Reviews. Neuroscience. 14(6): 417–428.

22. a, bAnagnostaras SG, Gale GD, Fanselow MS (2001). "Hippocampus and contextual fear conditioning: Recent controversies and advances." Hippocampus. 11(1): 8–17.

23. ^Bouton ME, King DA (1983). "Contextual control of the extinction of conditioned fear: tests for the associative value of the context." Journal of Experimental Psychology. Animal Behavior Processes. 9(3): 248–265.

24. a, bBouton ME, Bolles RC (1980). "Conditioned fear assessed by freezing and by the suppression of three different baselines." Animal Learning & Behavior. 8(3): 429–434.

25. ^Debiec J, LeDoux JE, Nader K (2002). "Cellular and systems reconsolidation in the hippocampus." Neuron. 36(3): 527–538.

26. ^Fanselow MS, Bolles RC (1979). "Naloxone and shock-elicited freezing in the rat." *Journal of Comparative and Physiological Psychology. 93(4): 736–744.*

27. a, b *Fendt M, Fanselow MS (1999). "The neuroanatomical and neurochemical basis of conditioned fear." Neuroscience and Biobehavioral Reviews. 23(5): 743–760.*

28. ^*Gewirtz JC, McNish KA, Davis M (2000). "Is the hippocampus necessary for contextual fear conditioning?" Behavioural Brain Research. 110(1–2): 83–95.*

29. ^*Holland PC, Bouton ME (1999). "Hippocampus and context in classical conditioning." Current Opinion in Neurobiology. 9(2): 195–202.*

30. ^*Kim JJ, Jung MW (2006). "Neural circuits and mechanisms involved in Pavlovian fear conditioning: a critical review." Neuroscience and Biobehavioral Reviews. 30(2): 188–202.*

31. a, b *Maren S, Holt W (2000). "The hippocampus and contextual memory retrieval in Pavlovian conditioning." Behavioural Brain Research. 110(1–2): 97–108.*

32. ^*Pezze MA, Feldon J (2004). "Mesolimbic dopaminergic pathways in fear conditioning." Progress in Neurobiology. 74(5): 301–320.*

33. a, b *Lovett-Barron M, Kaifosh P, Kheirbek MA, Danielson N, Zaremba JD, Reardon TR, Turi GF, Hen R, Zemelman BV, Losonczy A (2014). "Dendritic inhibition in the hippocampus supports fear learning." Science. 343(6173): 857–863.*

34. a, b *Rajasethupathy P, Sankaran S, Marshel JH, Kim CK, Ferenczi E, Lee SY, Berndt A, Ramakrishnan C, Jaffe A, Lo M, Liston C, Deisseroth K (2015). "Projections from neocortex mediate top-down control of memory retrieval." Nature. 526(7575): 653–659.*

35. ^*Leaf RC, Leaf SR (1966). "Recovery time as a measure of degree of conditioned suppression." Psychological Reports. 18(1): 265–266.*

36. ^*Leaf RC, Muller SA (1965). "Simple method for CER conditioning and measurement." Psychological Reports. 17(1): 211–215.*

37. a, b, c, d *Ratigan HC, Krishnan S, Smith S, Sheffield MEJ (2023). "A thalamic-hippocampal CA1 signal for contextual fear memory suppression, extinction, and discrimination." Nature Communications. 14(1): 6758.*

38. a, b, c, d *Krishnan S, Sheffield MEJ (2023). "Reward Expectation Reduces Representational Drift in the Hippocampus." In bioRxiv (p. 2023.12.21.572809). doi:10.1101/2023.12.21.572809.*

39. a, b *Ramanathan KR, Ressler RL, Jin J, Maren S (2018). "Nucleus Reuniens Is Required for Encoding and Retrieving Precise, Hippocampal-Dependent Contextual Fear Memories in Rats." The Journal of Neuroscience: The Official Journal of the Society for Neuroscience. 38(46): 9925–9933.*

40. a, b, c*Russo AS, Parsons RG (2021). "Behavioral expression of contextual fear in male and female rats." Frontiers in Behavioral Neuroscience. 15: 671017.*

41. a, b*Trott JM, Hoffman AN, Zhuravka I, Fanselow MS (2022). "Conditional and unconditional components of aversively motivated freezing, flight and darting in mice". ELife. 11. doi:10.7554/eLife.75663.*

42. a, b, c*Chu A, Gordon NT, DuBois AM, Michel CB, Hanrahan KE, Williams DC, Anzellotti S, McDannald MA (2024). "A fear conditioned cue orchestrates a suite of behaviors in rats." ELife. 13. doi:10.7554/eLife.82497.*

43. a, b*Dos Santos Corrêa M, Vaz BDS, Grisanti GDV, de Paiva JPQ, Tiba PA, Fornari RV (2019). "Relationship between footshock intensity, post-training corticosterone release and contextual fear memory specificity over time." Psychoneuroendocrinology. 110(104447): 104447.*

44. a, b*Navarro-Sánchez M, Gil-Miravet I, Montero-Caballero D, Castillo-Gómez E, Gundlach AL, Olucha-Bordonau FE (2024). "Some key parameters in contextual fear conditioning and extinction in adult rats." Behavioural Brain Research. 462: 114874.*

45. a, b, c, d*Poulos AM, Mehta N, Lu B, Amir D, Livingston B, Santarelli A, Zhuravka I, Fanselow MS (2016). "Conditioning- and time-dependent increases in context fear and generalization." Learning & Memory. 23(7): 379–385.*

46. a, b, c*Totty MS, Warren N, Huddleston I, Ramanathan KR, Ressler RL, Oleksiak CR, Maren S (2021). "Behavioral and brain mechanisms mediating conditioned flight behavior in rats". Scientific Reports. 11(1): 8215.*

47. ^*Baldi E, Lorenzini CA, Bucherelli C (2004). "Footshock intensity and generalization in contextual and auditory-cued fear conditioning in the rat." Neurobiology of Learning and Memory. 81(3): 162–166.*

48. ^*Cordero MI, Merino JJ, Sandi C (1998). "Correlational relationship between shock intensity and corticosterone secretion on the establishment and subsequent expression of contextual fear conditioning." Behavioral Neuroscience. 112(4): 885–891.*

49. ^*Daviu N, Molina P, Nadal R, Belda X, Serrano S, Armario A (2024). "Influence of footshock number and intensity on the behavioral and endocrine response to fear conditioning and cognitive fear generalization in male rats." Progress in Neuro-Psychopharmacology & Biological Psychiatry. 135(111112): 111112.*

50. ^*Quinn JJ, Wied HM, Ma QD, Tinsley MR, Fanselow MS (2008). "Dorsal hippocampus involvement in delay fear conditioning depends upon the strength of the tone-footshock association." Hippocampus. 18(7): 640–654.*

51. ^*Biedenkapp JC, Rudy JW (2007). "Context preexposure prevents forgetting of a contextual fear memory: implication for regional changes in brain activation patterns associated with recent and remote memory tests." Learning & Memory (Cold Spring Harbor, N.Y.). 14(3): 200–203.*

52. ^Rudy JW, Barrientos RM, O'Reilly RC (2002). "Hippocampal formation supports conditioning to memory of a context." *Behavioral Neuroscience.* 116(4): 530–538.

53. ^a, ^b Wiltgen BJ, Silva AJ (2007). "Memory for context becomes less specific with time". *Learning & Memory (Cold Spring Harbor, N.Y.).* 14(4): 313–317.

54. ^McNally GP, Westbrook RF (2006). "A short intertrial interval facilitates acquisition of context-conditioned fear and a short retention interval facilitates its expression." *Journal of Experimental Psychology. Animal Behavior Processes.* 32(2): 164–172.

55. ^Williams DA (1994). "Slow extinction of conditioned responding following exposure to two bouts of massed shock". *Animal Learning & Behavior.* 22(2): 203–213.

56. ^a, ^b Ji J, Maren S (2007). "Hippocampal involvement in contextual modulation of fear extinction." *Hippocampus.* 17(9): 749–758.

57. ^a, ^b Liu X, Ramirez S, Pang PT, Puryear CB, Govindarajan A, Deisseroth K, Tonegawa S (2012). "Optogenetic stimulation of a hippocampal engram activates fear memory recall." *Nature.* 484(7394): 381.

58. ^a, ^b Phillips RG, LeDoux JE (1992). "Differential contribution of amygdala and hippocampus to cued and contextual fear conditioning." *Behavioral Neuroscience.* 106(2): 274–285.

59. ^Ramirez S, Liu X, Lin PA, Suh J, Pignatelli M, Redondo RL, Ryan TJ, Tonegawa S (2013). "Creating a False Memory in the Hippocampus." *Science.* 341(6144): 387–391.

60. ^O'Keefe J, Dostrovsky J (1971). "The hippocampus as a spatial map. Preliminary evidence from unit activity in the freely-moving rat." *Brain Research.* 34(1): 171–175.

61. ^a, ^b Blair GJ, Guo C, Wang S, Fanselow MS, Golshani P, Aharoni D, Blair HT (2023). "Hippocampal place cell remapping occurs with memory storage of aversive experiences." *ELife.* 12. doi:10.7554/eLife.80661.

62. ^Kim EJ, Park M, Kong M-S, Park SG, Cho J, Kim JJ (2015). "Alterations of hippocampal place cells in foraging rats facing a 'predatory' threat." *Current Biology: CB.* 25(10): 1362–1367.

63. ^Kinsky NR, Orlin DO, Ruesch EA, Diba K, Ramirez S (2023). "Erasable hippocampal neural signatures predict memory discrimination." *BioRxiv.Org: The Preprint Server for Biology.* 2023.02.02.526824.

64. ^Mamad O, Agayby B, Stumpp L, Reilly RB, Tsanov M (2019). "Extrafield activity shifts the place field center of mass to encode aversive experience." *ENeuro.* 6(2): ENEURO.0423-17.2019.

65. ^a, ^b, ^c Moita MAP, Rosis S, Zhou Y, LeDoux JE, Blair HT (2004). "Putting fear in its place: remapping of hippocampal place cells during fear conditioning." *The Journal of Neuroscience: The Official Journal of the Society for Neuroscience.* 24(31): 7015–7023.

66. ^Ormond J, Serka SA, Johansen JP (2023). "Enhanced Reactivation of Remapping Place Cells during Aversive Learning." The Journal of Neuroscience: The Official Journal of the Society for Neuroscience. 43(12): 2153–2167.

67. a, b, c, d, eSchuette PJ, Reis FMCV, Maesta-Pereira S, Chakerian M, Torossian A, Blair GJ, Wang W, Blair HT, Fanselow MS, Kao JC, Adhikari A (2020). "Long-Term Characterization of Hippocampal Remapping during Contextual Fear Acquisition and Extinction." The Journal of Neuroscience: The Official Journal of the Society for Neuroscience. 40(43): 8329–8342.

68. a, bWang ME, Wann EG, Yuan RK, Álvarez MMR, Stead SM, Muzzio IA (2012). "Long-term stabilization of place cell remapping produced by a fearful experience". The Journal of Neuroscience: The Official Journal of the Society for Neuroscience. 32(45): 15802–15814.

69. a, bWang ME, Yuan RK, Keinath AT, Ramos Álvarez MM, Muzzio IA (2015). "Extinction of Learned Fear Induces Hippocampal Place Cell Remapping". The Journal of Neuroscience: The Official Journal of the Society for Neuroscience. 35(24): 9122–9136.

70. ^Wu C-T, Haggerty D, Kemere C, Ji D (2017). "Hippocampal awake replay in fear memory retrieval". Nature Publishing Group. 20(4): 571–580.

71. ^Colgin LL, Moser EI, Moser M-B (2008). "Understanding memory through hippocampal remapping." Trends in Neurosciences. 31(9): 469–477.

72. ^Leutgeb S, Leutgeb JK, Barnes CA, Moser EI, McNaughton BL, Moser M-B (2005). "Independent codes for spatial and episodic memory in hippocampal neuronal ensembles." Science (New York, N.Y.). 309(5734): 619–623.

73. ^Muller RU, Kubie JL (1987). "The effects of changes in the environment on the spatial firing of hippocampal complex-spike cells." Journal of Neuroscience. 7(7): 1951–1968.

74. ^Chen T-W, Wardill TJ, Sun Y, Pulver SR, Renninger SL, Baohan A, Schreiter ER, Kerr RA, Orger MB, Jayaraman V, Looger LL, Svoboda K, Kim DS (2013). "Ultrasensitive fluorescent proteins for imaging neuronal activity." Nature. 499(7458): 295–300.

75. ^Sheffield MEJ, Adoff MD, Dombeck DA (2017). "Increased Prevalence of Calcium Transients across the Dendritic Arbor during Place Field Formation." Neuron. 96(2): 490–504.e5.

76. ^Ramanathan KR, Maren S (2019). "Nucleus reuniens mediates the extinction of contextual fear conditioning." Behavioural Brain Research. 374(112114): 112114.

77. ^Totty MS, Tuna T, Ramanathan KR, Jin J, Peters SE, Maren S (2023). "Thalamic nucleus reuniens coordinates prefrontal-hippocampal synchrony to suppress extinguished fear". Nature Communications. 14(1): 6565.

78. ^Troyner F, Bicca MA, Bertoglio LJ (2018). "Nucleus reuniens of the thalamus controls fear memory intensity, specificity and long-term maintenance during consolidation". Hippocampus. 28(8): 602–616.

79. ^Vetere G, Kenney JW, Tran LM, Xia F, Steadman PE, Parkinson J, Josselyn SA, Frankland PW (2017). "Chemogenetic Interrogation of a Brain-wide Fear Memory Network in Mice". Neuron. 94(2): 363–374.e4.

80. ^Xu W, Südhof TC (2013). "A neural circuit for memory specificity and generalization". Science. https://science.sciencemag.org/content/339/6125/1290.short?casa_token=QtgiZVpOOvgAAAAA:1evZSg4yR3MKpHHsrcyiJs135dikEsxBXNlOZAipkPQiXbkaIkhokkaVVO3qDwmtWTIkwSzbdcZtbbE.

81. ^Tovote P, Fadok JP, Lüthi A (2015). "Neuronal circuits for fear and anxiety". Nature Reviews. Neuroscience. 16(6): 317–331.

82. ^Huckleberry KA, Ferguson LB, Drew MR (2016). "Behavioral mechanisms of context fear generalization in mice." Learning & Memory. 23(12): 703–709.

83. ^Maren, Holmes A (2016). "Stress and Fear Extinction." Neuropsychopharmacology: Official Publication of the American College of Neuropsychopharmacology. 41(1): 58–79.

84. ^Furuyama T, Imayoshi A, Iyobe T, Ono M, Ishikawa T, Ozaki N, Kato N, Yamamoto R (2023). "Multiple factors contribute to flight behaviors during fear conditioning." Scientific Reports. 13(1): 10402.

85. ^Dupin M, Garcia S, Messaoudi B, Doyère V, Mouly A-M (2020). "Respiration and brain neural dynamics associated with interval timing during odor fear learning in rats." Scientific Reports. 10(1): 17643.

86. ^Godsil BP, Quinn JJ, Fanselow MS (2000). "Body temperature as a conditional response measure for pavlovian fear conditioning." Learning & Memory. 7(5): 353–356.

87. ^Korn CW, Staib M, Tzovara A, Castegnetti G, Bach DR (2017). "A pupil size response model to assess fear learning." Psychophysiology. 54(3): 330–343.

88. ^Shionoya K, Hegoburu C, Brown BL, Sullivan RM, Doyère V, Mouly A-M (2013). "It's time to fear! Interval timing in odor fear conditioning in rats." Frontiers in Behavioral Neuroscience. 7: 128.

89. ^Stiedl O, Spiess J (1997). "Effect of tone-dependent fear conditioning on heart rate and behavior of C57BL/6N mice." Behavioral Neuroscience. 111(4): 703–711.

90. ^Datta SR, Anderson DJ, Branson K, Perona P, Leifer A (2019). "Computational Neuroethology: A Call to Action." Neuron. 104(1): 11–24.

91. ^Mathis MW, Mathis A (2020). "Deep learning tools for the measurement of animal behavior in neuroscience." Current Opinion in Neurobiology. 60: 1–11.

92. ^Syeda A, Zhong L, Tung R, Long W, Pachitariu M, Stringer C (2024). "Facemap: a framework for modeling neural activity based on orofacial tracking". Nature Neuroscience. 27(1): 187–195.

93. ^*Wiltschko AB, Tsukahara T, Zeine A, Anyoha R, Gillis WF, Markowitz JE, Peterson RE, Katon J, Johnson MJ, Datta SR (2020). "Revealing the structure of pharmacobehavioral space through motion sequencing". Nature Neuroscience. 23(11): 1433–1443.*

94. ^*Josselyn SA, Köhler S, Frankland PW (2015). "Finding the engram." Nature Reviews. Neuroscience. 16(9): 521–534.*

95. ^*Josselyn SA, Tonegawa S (2020). "Memory engrams: Recalling the past and imagining the future." Science. 367(6473). doi:10.1126/science.aaw4325.*

96. ^*Tonegawa S, Morrissey MD, Kitamura T (2018). "The role of engram cells in the systems consolidation of memory". Nature Reviews. Neuroscience. 19(8): 485–498.*

97. ^*Frankland PW, Josselyn SA, Köhler S (2024). "Engrams." Current Biology: CB. 34(12): R559–R561.*

98. a, b*Mocle AJ, Ramsaran AI, Jacob AD, Rashid AJ, Luchetti A, Tran LM, Richards BA, Frankland PW, Josselyn SA (2024). "Excitability mediates allocation of pre-configured ensembles to a hippocampal engram supporting contextual conditioned threat in mice." Neuron. 112(9): 1487–1497.e6.*

99. a, b*Monasterio A, Lienkaemper C, Coello S, Ocker GK, Ramirez S, Scott BB (2024). "CA1 Engram Cell Dynamics Before and After Learning." bioRxiv. doi:10.1101/2024.04.16.589790.*

100. a, b*Pettit NL, Yap E-L, Greenberg ME, Harvey CD (2022). "Fos ensembles encode and shape stable spatial maps in the hippocampus." Nature. doi:10.1038/s41586-022-05113-1.*

101. a, b*Suthard RL, Senne RA, Buzharsky MD, Diep AH, Pyo AY, Ramirez S (2024). "Engram reactivation mimics cellular signatures of fear". Cell Reports. 43(3): 113850.*

102. ^*Uytiepo M, Zhu Y, Bushong E, Polli F, Chou K, Zhao E, Kim C, Luu D, Chang L, Quach T, Haberl M, Patapoutian L, Beutter E, Zhang W, Dong B, McCue E, Ellisman M, Maximov A (2024). "Synaptic architecture of a memory engram in the mouse hippocampus". BioRxiv: The Preprint Server for Biology. doi:10.1101/2024.04.23.590812.*

103. a, b*Pachitariu M, Stringer C, Dipoppa M, Schröder S, Rossi LF, Dalgleish H, Carandini M, Harris KD (2017). "Suite2p: beyond 10,000 neurons with standard two-photon microscopy." BioRxiv. 061507.*

104. ^*Barth AM, Jelitai M, Vasarhelyi-Nagy MF, Varga V (2023). "Aversive stimulus-tuned responses in the CA1 of the dorsal hippocampus." Nature Communications. 14(1): 1–17.*

105. ^*Gruene TM, Flick K, Stefano A, Shea SD, Shansky RM (2015). "Sexually divergent expression of active and passive conditioned fear responses in rats." ELife. 4. doi:10.7554/eLife.11352.*

106. ^*Maren S, De Oca B, Fanselow MS (1994). "Sex differences in hippocampal long-term potentiation (LTP) and Pavlovian fear conditioning in rats: positive correlation between LTP and contextual learning." Brain Res*

*earch. 661(1–2): 25–34.*

107. ^*Aronov D, Tank DW (2014). "Engagement of Neural Circuits Underlying 2D Spatial Navigation in a Rodent Virtual Reality System." Neuron. 84(2): 442–456.*

## Declarations